Available online at www.sciencedirect.com

SCIENCE DIRECT®

Biochimica et Biophysica Acta 1666 (2004) 158–189

BIOCHIMICA ET BIOPHYSICA ACTA
BBA

http://www.elsevier.com/locate/bba

Review

Computer simulations of membrane proteins

Walter L. Ash[1], Marian R. Zlomislic, Eliud O. Oloo[1], D. Peter Tieleman*,[2]

Department of Biological Sciences, University of Calgary, 2500 University Dr. NW, Calgary AB, Canada T2N 1N4

Received 30 March 2004; accepted 29 April 2004
Available online 23 July 2004

Abstract

Computer simulations are rapidly becoming a standard tool to study the structure and dynamics of lipids and membrane proteins. Increasing computer capacity allows unbiased simulations of lipid and membrane-active peptides. With the increasing number of high-resolution structures of membrane proteins, which also enables homology modelling of more structures, a wide range of membrane proteins can now be simulated over time spans that capture essential biological processes. Longer time scales are accessible by special computational methods. We review recent progress in simulations of membrane proteins.

Keywords: Molecular dynamics simulation; Ion channel; Helix–helix interaction; Antimicrobial peptide; Bilayer structure; Outer membrane protein; Aquaporin

Contents

Abbreviations: MD, molecular dynamics; TMH, transmembrane helix; ns, nanosecond(s); ps, picosecond(s); DMTAP, 1,2-dimyristoyl-3-trimethylammonium-propane; DOTAP, 1,2-dioleoyl-3-trimethylammonium-propane; DOPC, 1,2-dioleoyl-*sn*-glycero-3-phosphocholine; DMPC, 1,2-dimyristoyl-*sn*-glycero-3-phosphocholine; DPC, dodecylphosphocholine; SDS, sodium dodecyl sulfate; POPE, 1-palmitoyl-2-oleoyl-*sn*-glycero-3-phosphoethanolamine; DPPC, 1,2-dipalmitoyl-*sn*-glycero-3-phosphocholine; POPC, 1-palmitoyl-2-oleoyl-*sn*-glycero-3-phosphocholine; GPCR, G-protein-coupled receptor; EM, electron microscopy; PMF, potential of mean force; *IV* curves, current–voltage curves; NBD, nucleotide binding domain; TMD, transmembrane domain; ABC, ATP binding casette

* Corresponding author. Tel.: +1 403 220 2966; fax: +1 403 289 9311.
E-mail address: tieleman@ucalgary.ca (D.P. Tieleman).
URL: http://moose.bio.ucalgary.ca.
[1] Supported by AHFMR studentships.
[2] Scholar of the Alberta Heritage Foundation for Medical Research (AHFMR).

0005-2736/$ - see front matter © 2004 Elsevier B.V. All rights reserved.
doi:10.1016/j.bbamem.2004.04.012

1. Introduction

In the last decade the availability of powerful computers has opened new ways to study lipid bilayers in atomic detail, yielding detailed pictures of the structure and dynamics of membranes and membrane proteins [1–6]. Increasing sophistication of models, software, and increasing computer power are now extending our reach beyond small patches of pure lipid on a nanosecond time scale to a wide range of problems on much longer time and length scales. The rapidly growing number of high-resolution structures of membrane proteins and increased knowledge of the principles of membrane protein structure have enabled computer simulations and modelling to become standard techniques to study membrane proteins in atomic detail.

Molecular dynamics simulations have developed over the last decades from a method to study the dynamics of liquids of solid spheres and Lennard–Jones particles to a versatile method to study a broad range of systems at atomic resolution. The basic method includes describing the interactions of all atoms in a given system by a relatively simple empirical potential function, from which the forces on all atoms can be calculated and integrated in time, using time steps of the order of 10^{-15} s. The primary result is a trajectory, which contains the motion of all atoms in time, over millions of time steps. Analysis of these motions gives insight into the system that is being studied [7].

What can we expect from molecular dynamics simulations of biological membranes? In principle, such simulations give complete details of the motions of lipids and other molecules in the system, and through those and statistical mechanics, access to thermodynamic properties. An example of a typical simulation system containing water, ions, phospholipids and a membrane protein is shown in Fig. 1. There are, however, major limitations. An important consideration for the use of simulation and to judge the reliability of simulations is the time and length scale on which the processes of interest occur. There also are technical limitations related to the accuracy of the empirical potential function, the relatively small size of the systems that can be simulated, and difficulties with accurately incorporating important variables such as pH, transmembrane potential differences, and low concentrations of ions. The starting configuration of a simulation may also bias the results in undesirable ways.

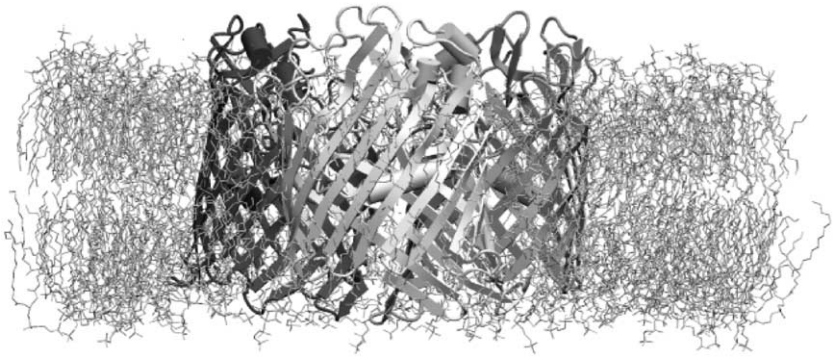

Fig. 1. A typical membrane protein simulation box. The box is only one cell in an infinite crystal due to the use of periodic boundary conditions to limit edge artefacts. Shown here is the *E. coli* outer membrane porin OmpF in its native trimeric state. Monomers are denoted with different scales of grey, and the bilayer (composed of a single phospholipid species) is shown in atomic detail as a stick representation. The bilayer is hydrated with water molecules and sodium chloride (not shown).

Several recent advances have contributed to a surge in the number of simulation studies appearing in the literature. Software is becoming more user-friendly, useful calculations can now be done on cheap and readily available computer hardware, and there is a rapidly growing number of high-resolution structures of membrane proteins that can be used for simulations and modelling. Methodological progress in force fields [8], parallel computer algorithms to improve sampling of motions that would normally be too slow to simulate (e.g., Refs. [9,10]), and algorithms to efficiently calculate electrostatic forces have also been critical in recent advances [11]. More progress in these areas can be expected, as free energy methods become more efficient and sampling methods adapted to massively parallel computers, such as ensemble dynamics [12] and replica exchange dynamics [9,13,14], are applied to problems involving membranes and membrane proteins.

In this review, we describe recent results and developments in simulations of membrane proteins. We start with a short summary of progress in simulations of pure lipids, followed by sections on different classes of membrane proteins.

2. Simulations of phospholipids

Accurate models of pure phospholipids are an essential component of membrane protein simulations, and are also important for understanding general principles of membrane organization and lipid chemistry. There has been significant progress in this area, both in improving the basic models and methods and in identifying bottlenecks for further development. Detailed reviews are available that cover older work [2,4–6]. We focus on studies from the last 2 years. Several recent studies have considered a bilayer of 128 lipids for 100 ns or longer, which turns out to be sufficient to accurately calculate translational diffusion coefficients of lipids in addition to a wide range of properties that equilibrate faster [15,16]. Simulations of bilayers of different sizes have helped understand the effects of finite size artefacts and have provided a first glance at larger-scale phenomena like undulations, which are effectively suppressed in simulations of small patches of lipid [17,18]. Another interesting development is the systematic application of MD simulations to a range of lipids, under a range of conditions including different temperatures, salt concentrations and electric fields. These now include a number of polyunsaturated lipids (e.g., Refs. [19–24]), with some exciting combinations between experiment and simulation, charged phosphatidylserine lipids [25–27], sphingomyelin [28–30], lipopolysaccharide [31], and cationic lipids such as DMTAP [32] and DOTAP (Leonenko et al., in preparation) which are used in DNA transfer. The sensitivity of the details of simulation results to force fields and simulation algorithms, however, makes it desirable to revisit some of these lipid simulations with the same force field and a consistent set of simulation algorithms to allow a more accurate direct comparison.

Simulations have also been used to investigate large-scale processes such as aggregation of lipids into bilayers and vesicles, electroporation, phase changes, and fusion. Aggregation of randomly dissolved phospholipids into bilayers takes on the order of tens of nanoseconds [33], whereas the formation of a small phospholipid vesicle has been observed in near-atomic detail in a simulation of ca. 100 ns [34]. Pore formation in bilayer models under the influence of electric fields or mechanical stress has been simulated [35–37], as well as membrane rupture by interactions with crystals [38]. Obvious next steps in this direction are to investigate pore formation by antimicrobial peptides or toxins, challenging problems that are now coming within reach of simulations. Cubic lipid phases have been studied by MD, and a phase transition between a cubic and an inverted hexagonal phase has been observed [39,40]. Such simulations might evolve to help understand a range of phenomena, including crystallization of membrane proteins using lipid cubic phases. Recent developments of so-called ‘coarse-grained’ force fields are quite promising for further studies of these large-scale processes [41–43], and have already been used to study bilayer and vesicle formation, structural features of inverted

hexagonal phases [42], vesicle fusion [44,45], and the distribution of different types of lipids in inner and outer leaflets of vesicles [46]. Both atomistic and coarse-grained simulations are beginning to reach into the mesoscopic domain, where properties calculated from detailed simulations can be compared to continuum mechanics concepts such as bending rigidities [36,47].

Biologically, charged lipids often make up 10–30% of a membrane, but never 100%. Simulations of mixtures remain difficult because of the long simulation times required to allow equilibration of mixtures of phospholipids [48,49]. The exact time required is not yet known, but it appears likely it will be hundreds of nanoseconds and possibly more. Alternatively, it might be possible to adopt more advanced sampling methods to equilibrate a mixture faster. Another area that has received significant attention concerns the properties of lipids in the presence of cholesterol [50–53]. Simulations of tens of nanoseconds are beginning to give reasonable statistical sampling of such interactions, although many older simulations explore local interactions only. The accurate representation of lipid mixtures will become an important problem as accessible time scales for membrane protein simulations increase; many protein properties strongly depend on lipid composition, which has so far been hard to capture accurately in simulations.

The interaction of small molecules with membranes was one of the first problems studied [6]. Recent work in this area concerns the accurate distribution of molecules of a significant size, the link between structure and physiological function (as in anaesthetics; Refs. [54,55]), and the relationship between shape, rigidity, and polarity and distribution in a lipid bilayer [26,56–58]. This type of calculation investigates problems that are interesting, but in addition provides a basis for improving the accuracy of protein parameters and sometimes allows a detailed comparison to experiment in order to validate the simulations [59]. Small molecules also modulate certain membrane proteins, and it will be important to get an accurate description of the interactions between all the components of such complex systems.

3. Simulations of peptides, small proteins, and viral proton channels

The folding of large membrane proteins, such as outer membrane porins, ion channels, photosynthetic and respiratory machinery, and G-protein-coupled receptors, is currently untenable by molecular dynamics simulations. The folding of moderately sized membrane proteins may occur on a time scale of microseconds, seconds, or even minutes, and simulations are just starting to reach beyond the nanosecond regime. The use of membrane mimetics such as slabs of hydrophobic molecules [60,61] and implicit solvent models [62–65] allows effectively longer simulations and can give useful results, though at the expense of a detailed view of the atomic interactions between proteins and lipids. Also, as the specific membrane environment is thought to affect the behaviour of some membrane proteins [21,66–68], fully detailed simulations are the most desirable in many cases. Most atomically detailed simulations have used pure, one-component phospholipid bilayers, although simulations of proteins in mixed lipid bilayers have also been done [69,70]. Simulations have also looked at the interactions of peptides with lipid monolayers [71–73] and with alkanethiol self-assembled monolayers [74].

Model peptides provide a link between the folding and behaviour of larger membrane proteins and simulations that are currently tractable. The fundamental properties and dynamics of transmembrane helices may be applicable to larger bundles, as current theories on membrane protein folding postulate that the α-helix is a fundamental folding domain for transmembrane α-helical bundle proteins [75,76]. One of the earliest attempts at modelling a folded transmembrane protein involved in vacuo molecular dynamics modelling of glycophorin A, an erythrocyte protein known to form dimers mediated by its single transmembrane domain [77]. More recent simulations have looked at fragments of larger proteins [78,79], membrane lytic antimicrobial peptides [80,81], and viral ion channels formed from homooligomeric assemblies of single transmembrane helices [82,83]. The latter two serve as models for understanding more complex proteins and channels in addition to being of biological and medical importance.

In this section we will discuss recent studies on the interfacial behaviour of membrane binding peptides including toxins and antibiotics, model transmembrane helices, and some interesting natural and synthetic ion channel forming peptides.

3.1. Membrane binding and interfacial folding

One interesting set of problems concerns the mechanism by which small peptides and peripherally associated membrane proteins bind to and interact with the water/membrane interface. A number of classes of these have been studied, including membrane lytic toxins, model peptides, fusion proteins, and peripherally associated signal transduction proteins and biosynthetic enzymes.

3.1.1. Membrane lytic peptides

Membrane lytic peptides are small (ca. 10–30 amino acids) amphipathic molecules, ubiquitous in nature, of which a large class are thought to act through a similar general mechanism which is not yet completely understood. It is proposed that these proteins can act by either coating the membrane and disrupting it by acting somewhat like a detergent, ultimately disintegrating it (the carpet, or Shai–Matsuzaki–Huang mechanism), or by forming transmembrane pores lined by peptides (the barrel-stave mechanism), thus starving the target cell for energy and nutrients [84,85].

Simulations have made some progress towards answering these questions. Because of their small size and the abundance of experimental information on them, these peptides have been useful models for refining membrane protein simulation methodology. Earlier work on melittin, alamethicin, dermaseptin-B, cecropin, magainin, and MB21 has been reviewed elsewhere [80,81,86].

Shepherd et al. [87] have investigated the mechanism of membrane binding and penetration of the membrane lytic amphipathic peptides dermaseptin S3 and MB21 on a DOPC bilayer. Membrane penetration required that the hydrophobic side of the peptides face the bilayer, causing significant disruption of membrane structure—in particular, a decrease in lipid acyl chain order and thinning of the bilayer (Fig. 2). This peptide-induced bilayer disorder provides some support

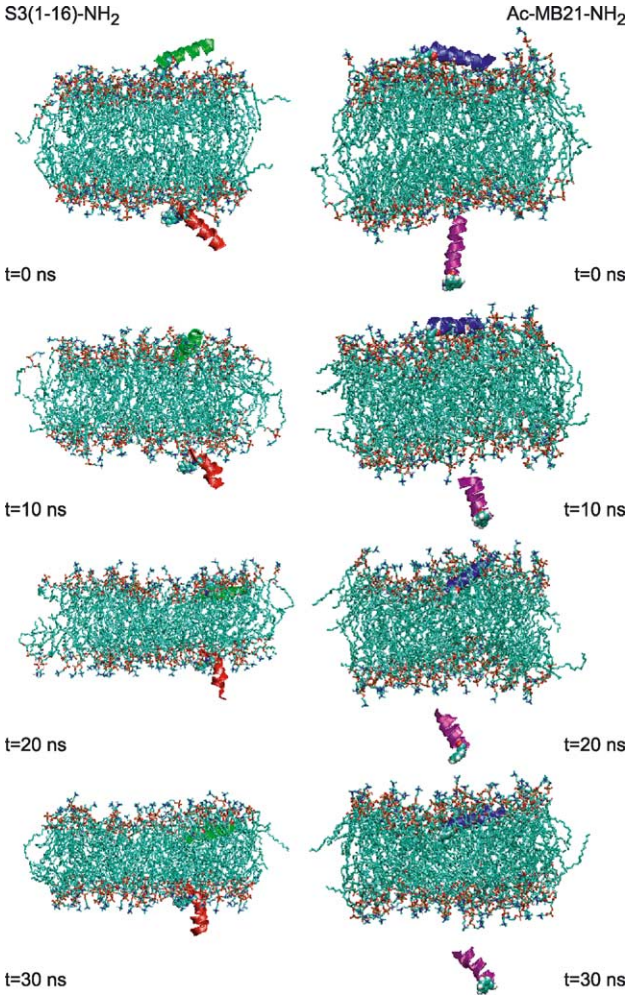

Fig. 2. The membrane lytic peptides dermaseptin S3 and MB21 cause thinning of a DOPC bilayer upon membrane binding, illustrated by this series of snapshots. Left: Truncated dermaseptin S3. Right: MB21. The peptides on the bottom and top faces of the membrane were oriented so that their hydrophilic and hydrophobic sides, respectively, were directed towards the membrane. When the hydrophobic face was directed towards the bilayer, binding occurred more readily and resulted in deeper penetration, demonstrating that acquisition of the proper orientation is an important part of membrane binding of these peptides. Reproduced with permission from Shepherd et al. [87]. © The Biochemical Society.

for the carpet model of antimicrobial activity. Bilayer association stabilized peptide α-helical secondary structure, and tryptophan residues were found to occupy interfacial regions of the bilayer, which is consistent with neutron-diffraction experiments on other tryptophan containing peptides. A series of simulations that restrained the peptide at different distances from the bilayer provided evidence for a detectable association energy. Previous simulations on the peptide sandostatin evidenced similar interactions [88]. Other studies have examined the synthetic lytic peptides LK9 and LK15 binding to DMPC monolayers [71].

Bombolittin is a peptide from bumblebee venom that folds into an α-helix in the presence of sodium dodecyl sulfate (SDS) micelles. Simulations of this peptide at a decane–water interface were done to support a model of peptide–lipid interactions from NMR studies in SDS micelles [89]. These NMR-based spin probe studies determined the accessibility of different side chains to hydrophobic and hydrophilic probe reagents. This mapping matched well with the hydrophobic burial profiles of side chains seen in the simulations, which were stable for 10 ns. Furthermore, a consistent orientation was reached within a few hundred picoseconds in simulations of peptides initially placed in agreement with the NMR data or by spontaneous reorientation of those oriented in conflict with it. Overall, the simulations and NMR results show bombolittin lies in α-helical conformation along the surface of a micelle (and by extension, probably a membrane) in a well-defined orientation.

Computer simulations are commonly used to interpret spectroscopic data. Huang et al. [90] used implicit solvent calculations on cobra cardiotoxin CTX A3 to interpret polarized attenuated total internal reflection infrared spectroscopy data, suggesting modes of binding of this toxin to zwitterionic and anionic membranes. This toxin appeared to have a greater thinning effect on anionic phosphatidylglycerol monolayers than on those composed of zwitterionic phosphatidylcholine species.

3.1.2. Interface associated, non-lytic peptides

A number of other membrane–water interface associated peptides have been investigated. Wong and co-workers studied the HIV fusion protein gp41 and mutants in POPE bilayers [91,92], with comparison between simulations and attenuated total internal reflection infrared spectroscopy to determine the orientation of peptides relative to the bilayer. The simulation component of this study involved the removal of several lipids from one leaflet in order to accommodate the protein inclusion. This points to a difficulty encountered when setting up all membrane protein simulations; it is hard to decide how many lipids should be placed in each leaflet in order to accommodate the protein inclusion without imparting unrealistic bilayer stress. Furthermore, the initial distribution of lipids between the two leaflets (whether symmetric or not) might subsequently affect the ability of a peptide to bind or acquire a new

orientation. Some authors have added a surface-binding peptide to both sides of a bilayer with equal leaflet composition in a single simulation, which might compensate for this effect [87,93], but this could neglect real effects caused by asymmetric interactions such as a peptide binding only to the outside of a cell. A recent study investigated the use of $P2_1$ and *Pc* space groups with periodic boundary conditions in simulations, including one of melittin in a DOPC bilayer [94]. This allowed lipids to move between the two leaflets simply by diffusing through one of the unit cell boundaries, and could compensate for errors in assigning initial conditions. Most simulation software in common use right now has not implemented this boundary condition, although it would be interesting to see more work done with it.

One recent study examined two pentapeptides with the sequence Ace-WLXLL, with X=Arg or Lys. These peptides were used by Wimley et al. [95] to examine the ability of salt bridge interactions to stabilize hydrophilic amino acids in a hydrophobic environment. Simulations investigated the behaviour of these peptides in different environments: water, octanol saturated with water, a water–hexane biphasic system, and a hydrated DOPC bilayer, which gave insight into important electrostatic interactions in these peptides and the interfacial behaviour of tryptophan [93]. An important role for tryptophan was also suggested by studies on the opioid peptide dynorphin [96,97]. Simulations with and without an N-terminal tryptophan suggested this residue kept the peptide in the interface, which might be necessary for receptor interaction. In another study, interfacial anchoring roles for the basic amino acids in pulmonary surfactant protein B were examined in fatty acid monolayers [73]. This protein is important in modulating surface tension in the alveolae of lungs, and simulations afforded some mechanistic insight into this capability.

Amphipathic peptides containing leucine and lysine have been studied at interfaces [98]. An older study examined the folding of a short polyleucine α-helix at the water–hexane interface, followed by transverse insertion into the hexane slab [99]. This is still one of very few examples of a simulation of the unassisted folding and insertion of a membrane-associated peptide. Zangi et al. [100] simulated the early stages of folding of the fungal hydrophobin SC3, a protein that can self-assemble into amphipathic layers at a hydrophobic/hydrophilic interface. Starting from an extended conformation, the protein was observed to fold into an amphipathic β-sheet-containing structure during a 135-ns simulation at a water–hexane interface. In contrast, simulations in hexane or water alone resulted in largely unstructured globules, suggesting interfaces may catalyze the rapid formation of secondary structure. This has been suggested by other simulations [98,99,101,102]. Folding and surface binding of small peptides has also been investigated in micelles [103,104].

3.1.3. Peripheral proteins

In addition to the small peptides and proteins already mentioned, several larger peripheral membrane proteins have been investigated by molecular dynamics. Nordgren et al. [74] looked at cytochrome *c* in association with different alkanethiol self-assembled monolayers, with the aim of understanding the structural features of the protein in these complexes and the nature of the monolayer association. An earlier work examined the proposed membrane anchoring domain of prostaglandin H2 synthase with the aid of continuum solvent calculations and explicit molecular dynamics with a DMPC bilayer [105]. A model for membrane association and catalytic site accessibility to lipid substrates was proposed, and a protein–lipid interaction similar to that predicted by simulation has since been observed in a high-resolution crystal structure of the protein solved in detergent [106]. Murray and co-workers have employed continuum electrostatics to examine the membrane association of phospholipase C [107] and FYVE domains [108]. Many peripherally associated proteins have important roles in signal transduction and disease, and simulations continue to be a powerful method to understand the detailed lipid–protein interactions responsible for their activity.

3.2. Transmembrane helix behaviour

Membrane spanning helices can be considered the smallest autonomous membrane protein domains [75,76]. Many simulations have been conducted on transmembrane helices; earlier progress in this area has been reviewed elsewhere [86]. These simulations can be done in order to study properties of fundamental interest, such as the dynamics of isolated helices [109,110], protein–lipid interactions [111,112], helix association [113], and the behaviour of simple channels such as those formed by certain fungal proteins and toxins [81]. Modelling protocols for predicting the native conformation of loops that link transmembrane domains have also been developed [114]. It may be eventually possible, with a few more years of increases in computer power and algorithm development, to completely understand membrane protein folding using computational techniques, although this ultimate goal is still far from realized.

3.2.1. Resolving ambiguities in TMH definition

Sequence analysis is one method by which transmembrane helices from membrane proteins can be identified. Different methods sometimes predict different transmembrane regions, and there is no clear way to identify correct predictions. Simulations offer an attractive way to refine TMH definitions, and have been applied to the transmembrane regions of Influenza A M2 protein [115], HIV VPU and Influenza B NB proteins [83]. More recently, the transmembrane helices from the gated potassium channels KcsA, Shaker [116], and Kir6.2 have been analyzed [117].

Experimental verification of precise transmembrane helix boundaries is very difficult.

MD simulations have also looked at the effects of hydrophobic mismatch on peptide and bilayer dynamics. Mismatch results when the effective hydrophobic thickness of the bilayer does not match that of a perfectly transmembrane-oriented helix [66]. Several mechanisms might compensate for this mismatch, including changes in peptide tilt, changes in secondary structure, peptide association, aggregation of different lipid species near the protein, and adaptation of bilayer structural properties like thickness or curvature. Petrache et al. [112] studied the WALP series of model peptides, which consist of a variable length leucine–alanine repeat flanked by terminal tryptophan residues. The peptides varied in length from 16 to 23 residues (approximately 2 to 3 nm in hydrophobic thickness), and were systematically examined in both DMPC and DPPC bilayers. It was found that both bilayers increased their thickness marginally with longer peptides. Specific bilayer deformations in the vicinity of the peptides could be observed, and subtle effects on protein–lipid packing that depended on the relative position of the flanking tryptophan residues around the helix axis were seen, a property that depends on the length of the intervening leucine–alanine repeat. This was quantified as a periodicity in the way WALP peptide length modulated a number of identified properties such as the interaction energy between the two monolayers and the helix tilt relative to the bilayer (Fig. 3). This modulation of protein–lipid interactions was particularly interesting because it demonstrated that even in these simplified model systems, hydrophobic mismatch is not the only factor influencing system behavior; a geometric effect should also be considered when interpreting experimental data.

3.2.2. Dynamics of proline-kinked helices, ion channel pore helices

The dynamic properties of individual helices can be examined in detail with MD. A number of proline and glycine-containing sequence motifs have been extensively studied. It appears that transmembrane helix flexibility mediated by specific sequence motifs could have important consequences for the activity of membrane proteins such as gated ion channels [78,118,119]. Proline and glycine are both thought to be important mediators of hinge-bending motions; proline disrupts normal helical hydrogen bonding and may participate in repulsive steric interactions with adjacent backbone atoms. Proline and glycine motifs were identified from analysis of a sequence database and simulated in polyalanine host helices [109], giving kink angles in reasonable agreement with those culled from a transmembrane helix structural database [120]. A related study on TMH-2 of the chemokine receptors identified a highly conserved TXP sequence motif by multiple sequence alignment [121]. MD simulations were employed to investigate the effects of this sequence on the behavior of polyalanine in a hydrophobic environment, suggesting hydroxyl-containing amino acids also modulate the kink behavior of proline-containing sequences. This prediction

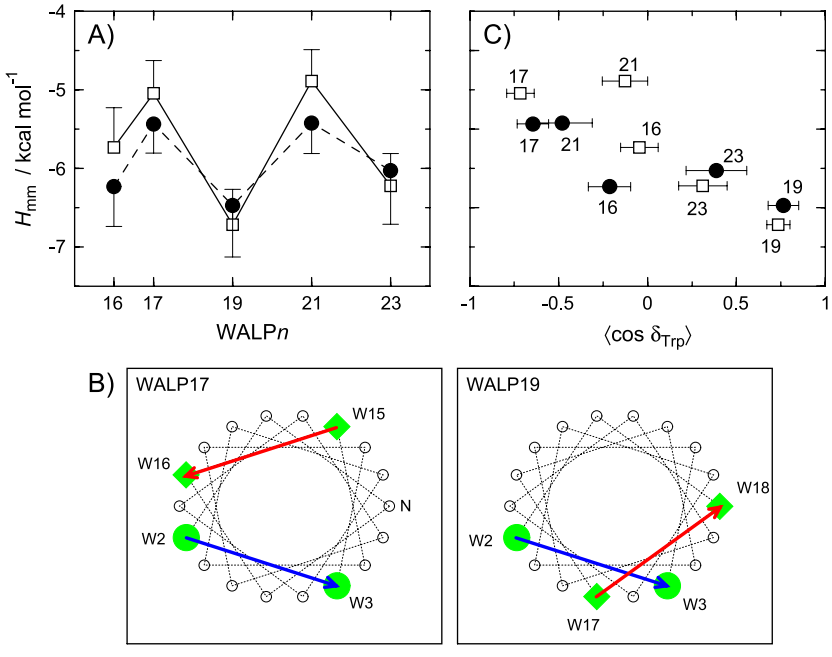

Fig. 3. (A) Interaction energy between membrane leaflets plotted versus WALP peptide length. Filled circles and open boxes denote DPPC and DMPC bilayers, respectively. (B) Helical wheel projections of WALP17 and WALP19 show that the length of the leucine–alanine repeat sequence changes the relative location of terminal tryptophan residues on the face of the helix. (C) The data from panel A plotted versus the average cosine of the angle between vectors shown in panel B. The horizontal bars indicate the mean square fluctuations of this property. Together these results indicate that bilayer structure is modulated by the location of interfacial tryptophan residues, and that bilayers are more rigid for WALP19 and WALP23 peptides with all tryptophans on the same side of the helix. Reprinted with permission from Petrache et al. [112].

was followed up by site-directed mutagenesis studies on the protein, demonstrating the importance of these two residues in ligand-mediated receptor activation. Further analysis of a non-redundant transmembrane helix sequence database showed the sequences SXP and TXP are overrepresented and simulations gave insight into the structural modulations mediated by these sequences [122]. Other studies on proline hinges in potassium channel helices have been conducted [116,117], all suggesting a similar role of proline and glycine motifs in mediating structural flexibility by providing a hinge connecting two relatively rigid helical segments. The second transmembrane segment of the nicotinic acetylcholine receptor δ-subunit is another kinked helix that has been examined [123,124], and this peptide has been subjected to continuum calculations [64,125].

3.2.3. SNARE proteins and membrane fusion

The viral fusion protein gp41 has been mentioned previously in this review (see above). Many other proteins and peptides are known to promote membrane fusion, although exactly how this happens remains an enigma [126]. In eukaryotes, a particularly important class of fusion proteins is the SNARE proteins [127]. These are involved in vesicular transport in which membrane fusion is mediated by the formation of SNARE complexes between vesicle and target membrane associated SNARE proteins. The SNARE complex involved in synaptic exocytosis is one of the best characterized, comprising the proteins syntaxin 1a and SNAP-25 on the plasma membrane, and synaptobrevin 2 on the synaptic vesicle membrane.

A recent set of simulations addressed the question of whether or not syntaxin 1A is capable of actively mediating membrane fusion, by examining the properties of a linker that connects its transmembrane domain to the cytoplasmic domain [70]. The protein was embedded independently in each of a binary mixture of zwitterionic lipids and an anionic ternary mixture. Free energy estimates from these simulations allowed the stiffness of the linker to be determined for both wild-type and mutant SNARE proteins, suggesting that a single SNARE protein could provide around 1 kcal/mol of energy to overcome repulsion between fusing membranes and deformation of the membrane. As multiple SNARE proteins are thought to be involved in the formation of a membrane fusion pore [128], these results suggest SNARE proteins could actively mediate membrane fusion.

3.2.4. Helix–helix interactions

The interaction between α-helices is thought to be one of the most important determinants of membrane protein structure and function [75,129]. Proteins comprising pairs of α-helices can be employed as models for understanding these interactions. One approach is to model and evaluate interactions between pairs of helices with techniques such as simulated annealing and global searching molecular dynamics [77,130–133] or Monte-Carlo simulations [134], either with an all-atom MD force field [135] or a simplified interaction potential function [136]. One of the more recent examples of the latter involved the correct prediction of the glycophorin A transmembrane fold [136]. This was followed by an as-yet unverified, but experimentally consistent, prediction for the transmembrane-domain mediated activation of the erbB2/neu receptor tyrosine kinase [137]. Efforts have been made to understand the nature of sequence-independent driving forces for helix-interactions [138–140], although the importance of these effects is not yet fully understood. A detailed review of these interesting studies is beyond the scope of this article.

3.3. Viral and other small ion channels

Viral ion channels are formed from small proteins (60–120 amino acids) that play several important roles in the lifecycle of some viruses [141]. As some of the simplest channels known, they have even gained attention in the context of the origins of membrane proteins during early evolution of the biosphere [142]. Much of the simulation work on these channels has been reviewed recently [82,143].

Many small channels that conduct protons have been identified, including gramicidin A [144], the influenza A M2 channel [145], and the engineered LS2 channel [146]. Proton transport presents a special challenge to molecular dynamics simulations because protons move between different water molecules and are not easily treated by a classical potential function. In the past few years, several different approaches have been developed for studying proton transport in membrane proteins. Several papers by Pomes and coworkers have investigated proton transport through gramicidin A and derivatives using the PM6 water model [144,147,148]. PM6 is a polarizable and dissociable empirical water model consisting of O^{2-} and H^{+} moieties [149]. Voth and coworkers have applied a different method to model proton channels like LS2 [150] and to models of the Influenza A M2 channel [150,151]. This model is based on the empirical valence bond (EVB) theory of Warshel [152]. LS2 is a synthetic peptide consisting solely of serines and leucines that forms tetrameric proton-permeable helix bundles [146]. Models of LS2 have been built by several groups [153,154], but critical comparison of these models with experimental conductance data has been difficult. We will return to proton transport in the context of aquaporins.

3.3.1. Alamethicin

Alamethicin is a member of the peptaibol family of pore forming peptides. It only has 20 residues but has the interesting property that it forms well-defined channels with reproducible conductance levels [155]. A model for transmembrane channel assembly involves several stages including membrane binding, transmembrane reorientation or insertion, and bundle association, all of which can—at least in principle—be simulated. Transmembrane reorientation of a surface bound peptide is perhaps the most difficult to

observe in a real bilayer due to slow membrane dynamics, although this has been observed at an octane/water interface [156].

Alamethicin has been particularly useful as a model for studying protein–membrane interactions and ion channel function, both computationally and experimentally [157,158]. Several recent papers have tested simulation methods on models of alamethicin channels, in particular the effects of different treatments of long-range interactions [159,160]. Tieleman et al. concluded that the PME method, a form of lattice sum, is most accurate and does not seem to suffer from periodicity artefacts as observed in some other test cases. In particular, periodicity artefacts are expected to become smaller as more water and larger bilayers are used, but this was not observed. In contrast, Bostick et al. compared 3D PME with a 2D method and found strong artefacts in the 3D case. The results of these two papers, on exactly the same alamethicin model, are not consistent but this will no doubt continue to be the subject of more investigations, as the treatment of electrostatic interactions in simulations is an important technical detail. Simulations have also been used to attempt to assign aggregation states to experimentally observed conductance levels. Based on indirect arguments, it seems likely the smallest observable conductance level corresponds to a pentameric arrangement of alamethicin monomers [160]. Recent progress in Brownian dynamics simulations suggests that applying such calculations on models generated by MD simulations will provide a more direct link soon. A 100-ns simulation of a model of six alamethicin helices is one of the longest ion channel simulations to date and showed that the model is quite stable on that time scale [161]. Alamethicin has also been used to develop continuum electrostatic calculations that are computationally much cheaper than fully atomistic simulations. A comparison of alamethicin channel structures from MD simulations in their stability with those estimated with continuum models suggested several discrepancies that provide interesting starting points for further studies [162]. These discrepancies may be the result of inaccuracies in either the continuum model or the MD force field, or may be a result of the slow dynamics of lipid bilayers that might not allow instability to be revealed by MD without longer simulations. Finally, alamethicin and related peptides can be synthesized and modified at will. Starostin et al. [163] designed an alamethicin version that shows pH-dependent selectivity. Model building and simulations of this peptide explain that the maximum anion vs. cation selectivity is limited due to counter-ions binding to charged sites in the channel. Simulations predicted a salt-concentration-dependent selectivity, which was verified experimentally [164].

4. Bacteriorhodopsin and G-protein-coupled receptors

Bacteriorhodopsin and rhodopsin are both seven-transmembrane retinylidene-containing membrane proteins, which are functionally different in spite of their similar architecture [165] and photochemistry [166]. When detailed structural information about bacteriorhodopsin was made available, it became the basis for a number of homology models of G-protein-coupled receptors (GPCRs), also known as heptahelical (7-TMH) transmembrane proteins. Improved structural resolution from a variety of experiments [167], culminating in a 2.8-Å resolution X-ray crystal structure of bovine rhodopsin [168], clearly demonstrated that these proteins were quite different in spite of their similar architecture, and that bacteriorhodopsin should not be used as a template for homology modelling of GPRCs. The GPCR protein family represents 1–3% of genes encoded by the human genome, and their functions represent a broad array of physiological processes that are of interest in pharmaceutical research. As rhodopsin is the only member of this protein class to have high-resolution crystal structures available [168], many homology models of other GPCRs have been built based on rhodopsin and used in docking and ligand binding studies [169–180]. Studies of rhodopsin and other GPCRs based on the rhodopsin structure have recently been reviewed [171,172,176,177]. Rhodopsin has also served as a model case for the development of algorithms to predict the conformation of loops connecting helices in transmembrane proteins [114].

Besides the seven-transmembrane helices characteristic of GPCRs, the high-resolution X-ray crystal structure of bovine rhodopsin showed features not found in bacteriorhodopsin, including a beta-strand cap in the extracellular environment between helices 3 and 4, and an eighth amphipathic helix at the cytoplasmic interface that contains two palmitoylation sites. These features are illustrated in Fig. 4. Many simulation studies have aimed to understand how changes in the retinal chromophore, buried between the TM helices, affect the local and global protein structure, and how these changes are coupled to activation of the G-proteins, which in turn amplify the signal to the cell.

In the dark-state (inactive) rhodopsin, retinal is in an 11-*cis* conformation. Activation is accomplished by isomerization of retinal to the all-*trans* isomer, which in turn evokes a response by the G-protein to which it is coupled. The complete photocycle of rhodopsin occurs on the order of milliseconds. Despite the fact that millisecond processes cannot yet be studied by atomistic molecule dynamics, extensive work with rhodopsin has been done to shed light onto the photochemistry of this protein [166]. Simulations published to date focus on understanding the global protein environment [181] and how isomerization of retinal affects the local protein environment in the binding pocket which leads to signalling [182,183]. A recent 40-ns simulation of rhodopsin in an explicit POPC bilayer and water system focused on studying cooperative interactions and transitions in the system, such as helix–lipid interactions, hydrogen bond networks, and salt bridges, all in the absence of a stimulus [181]. Simulations that have

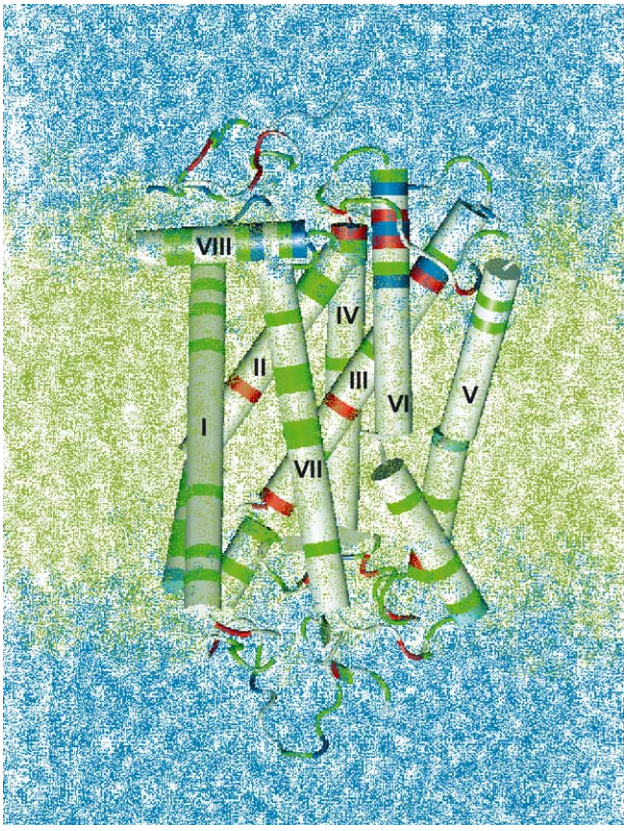

Fig. 4. Cartoon diagram of rhodopsin highlighting the characteristic seven-transmembrane helix architecture of G-protein-coupled receptors. The lipid bilayer is colored tan and water is colored blue. The top of the figure corresponds to the cytoplasmic face of the membrane, and is the location of the eighth helix (labelled VIII) in rhodopsin that is not observed in bacteriorhodopsin. Reproduced with permission from Crozier et al. [181].

isomerized the retinal chromophores from 11-*cis* to all-*trans* have observed resultant structural rearrangements of the helices on the nanosecond time scale [182,183]. Considering the time scale and size limitations already imposed by the system, rearrangements observed in the protein core appear reasonable, but a complete transition between inactive and activated rhodopsin has not yet been observed. Experimental results have been amalgamated (and subjected to molecular dynamics simulations) to develop a model of meta-rhodopsin II, the activated form of rhodopsin [184]. Although the behavior of the core of the protein appears to be similar regardless of whether a membrane mimetic such as hexane or a POPC bilayer is used [182,183], rhodopsin is known to be sensitive to the lipid environment. Simulations have been conducted which suggest a preferential solvation of rhodopsin by particular lipid species [21]. Studies aiming to understand a complete transition between the inactive and active forms of rhodopsin might therefore show a strong dependence on the exact nature of the lipid environment.

Simulations of bacteriorhodopsin have aimed to determine how changes in the conformation of the retinal moiety contribute to the function of the protein as a proton pump. The first structure of bacteriorhodopsin became available in 1990 [185] from cryo-electron microscopy with a resolution of 3.5 Å in the membrane plane, and 10-Å resolution in the perpendicular plane. At this resolution, assignment of the identities of the transmembrane helices could be made. In the earliest simulation of the entire bacteriorhodopsin protein, Nonella and et al. [186] completed the model of bacteriorhodopsin, and subjected the model to 20-ps molecular dynamics simulations in vacuum. Another early simulation of bacteriorhodopsin compared the protein in vacuum and lipid bilayer environments in 300-ps simulations [187]. Since that early work, increases in computer power and advances in simulation techniques have made QM/MM ab initio or semi-empirical treatments of the bacteriorhodopsin photocycle feasible [188].

5. Aquaglyceroporins

The aquaglyceroporin superfamily consists of membrane proteins that primarily facilitate the passive diffusion of water and other small neutral molecules, and have been identified in all forms of life. The aquaporin water channel AQP1 and the glycerol facilitator GlpF are two model systems from this superfamily that have been examined in detail. AQP1 is permeable to water but not protons or ions; GlpF channels glycerol (and similar substances) and is less permeable to water than AQP1. Cryo-EM and X-ray crystal structures of AQP1 [189,190] from red blood cells and GlpF [191] from *Escherichia coli* have shown that these proteins exist as tetramers in the membrane, and each monomer forms a separate water channel (Fig. 5A). A monomer consists of six transmembrane helices in an "hourglass" arrangement, and has two loops that dip into the protein from each side of the membrane. These re-entrant loops have a conserved coil–NPA–helix motif, where the Asn–Pro–Ala (NPA) residues of the two loops meet at the centre of the protein pore (Fig. 5A, between helices HB and HE). The GlpF structure has a high affinity glycerol binding site at one entrance and a so-called "greasy slide"—a hydrophobic lining that is absent in AQP1. A comparison of the structural features of the available aquaglyceroporin structures as of 2003 has been presented by De Groot et al. [192], and progress in simulations of aquaporins has been the subject of recent reviews [10,193–195]. Simulations of the aquaglyceroporins are particularly interesting because the time scale at which these membrane proteins perform their natural function—the conduction of water and/or glycerol—is on the order of nanoseconds. This time scale is easily accessible by the current state of the art in molecular dynamics simulations.

5.1. Water in aquaporins

The aquaporin structure is illustrated in Fig. 5A [196], which highlights important regions including the re-entrant

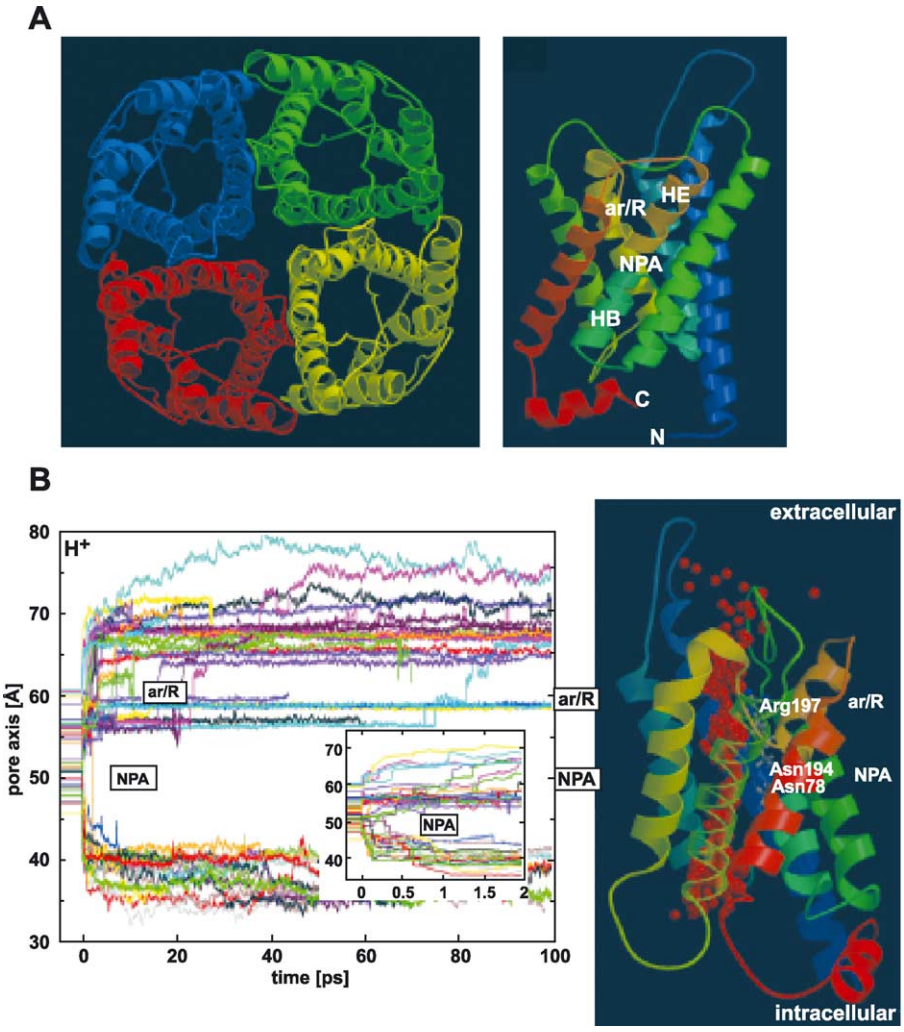

Fig. 5. Structure and mechanism of proton exclusion from aquaglyceroporins. (A) The water channel aquaporin (AQP1) forms a tetramer (shown from above), and each monomer forms a water channel through the membrane. A side view of a single monomer shows the re-entrant loop helices HB and HE, the NPA motif, and the ar/R region. (B) A one-dimensional projection of the trajectories of protons through the pore of aquaporin from a Q-HOP simulation shows that protons are excluded from the region of the pore near the NPA motif and to a lesser extent the ar/R region. These regions are highlighted in the structure to the right; red spheres denote regions in which proton hops occurred. The starting positions of the protons are shown by horizontal lines on the left portion of the graph. Panel A reproduced with permission from de Groot et al. [192]. Panel B from de Groot et al. [196].

loop helices HB and HE, the NPA motif, and the constriction (ar/R) region where the presence of a pair of aromatic residues and an arginine residue decreases the radius of the pore. In the last few years, a large number of interesting simulation studies on both AQP1 and GlpF have appeared. In the most recent studies, high-resolution crystal structures used as starting structures for simulations have stable secondary, tertiary and quaternary structures, although the first simulations of AQP1 suffered from starting structures that had poorly resolved side chains of residues in the channel, particularly at the NPA motif [197,198]. In a simulation using the highest resolution structure of AQP1 available at the time, Zhu et al. [198] observed that the water file in the channel was broken by interactions with side chains in the pore near the NPA motif. Simulations of a structure in which this region was modeled against the configuration observed in the better resolved GlpF crystal structure showed an unbroken line of water molecules [197]. In this work, the low-resolution EM structure was refined using a combination of homology modelling on GlpF and simulations that incorporated electron density directly as a constraint. The resulting AQP1 model (Protein Data Bank entry 1H6I) agreed remarkably well with the high-resolution crystal structure published later and formed the basis of subsequent simulation studies described below.

Simulations [199,200] based on different structures of AQP1 [197] and GlpF [191,200] with improved resolution illustrated the permeation of contiguous water chains through the AQP and GlpF pores. Although classical MD simulations neglect quantum mechanical effects and do not consider protons, disruption of the hydrogen bonding patterns of the water files in these simulations could be interpreted, suggesting possible mechanisms of proton

exclusion by these water channels. Over the course of 10-ns simulations, de Groot and Grubmuller [199] observed full permeation events of water molecules through the AQP1 channel, accompanied by a change in the dipole orientation of water molecules as they traversed the protein. This dipole inversion was thought to result from dipole–dipole interactions between water molecules and the re-entrant loop helices, in addition to an electrostatics-enforced orientation of the water molecule at the inversion site. Furthermore, the region of the pore near the NPA motif was thought to act as a selectivity filter, suggested by a comparison of this region between AQP1 and GlpF. Proton exclusion was proposed to result primarily from water chain disruption by the ar/R region, and electrostatic repulsion with the positively charged arginine. An interesting result from the simulations of GlpF, in which the crystallographic glycerol molecules were deleted in the MD starting structure, was the observation that the size of the pore diminished with time, suggesting that the size of the pore (particularly around the NPA motif) has an "induced fit" gating motion which accommodates the transport of glycerol, but reduces the rate of diffusion of other species like water.

Tajkhorshid et al. [200] studied water conduction through glyceroporins, in an interesting study combining crystallographic characterization of wild-type GlpF (with and without crystallographic glycerol molecules) and a mutant GlpF (with mutations in the region this group calls the "selectivity filter") with MD simulations. Analysis of these simulations allowed them to make a compelling argument that enforcing a water dipole inversion serves as the primary proton exclusion mechanism by restricting the formation of a proton wire, without breaking the continuous chain of water molecules. A physically unrealistic but informative modification to the simulation parameters, whereby electrostatic contributions from the NPA motif and the backbone atoms of the re-entrant helices were turned off [200,201], resulted in a breakdown of this dipole inversion and the formation of a regular water wire, demonstrating the importance of these motifs. Electrostatic interactions with the conserved arginine in the ar/R region were not considered strong enough to restrict proton passage, and a continuous water file was observed in this region. Methods to quantify water conduction properties such as osmotic permeability of AQP via MD simulation methods have also been developed. These methods involve inducing a hydrostatic pressure difference across a membrane with embedded AQP [202,203].

Studies addressing glycerol conduction through the GlpF protein have made use of classical and steered MD. Jensen and et al. [204] observed spontaneous, one-dimensional diffusion of glycerol and water through the GlpF channel. Transport of both species is correlated as they compete for hydrogen-bonding partners simultaneously. The backbone oxygen atoms in the coil (or non-helical) portions of the re-entrant loops were observed to form hydrogen bonds with the glycerol molecules. The non-helical segments of each loop are stabilized internally by hydrogen bonds between the backbone amide groups and an important glutamate residue. The structural stability and hydrogen bonding capacity of the NPA motif in the presence of passing substrates were observed in these simulations. Steered MD simulations were employed to study the conduction pathway of a single glycerol molecule in each channel of tetrameric GlpF by the application of either constant force or constant velocity to the glycerol centre of mass [205]. A free energy profile or potential of mean force (PMF) was reconstructed along the conduction pathway, identifying binding sites and barriers in the channel. The periplasmic entrance to GlpF was identified as a low energy site, which may contribute to efficient glycerol uptake from the periplasm. The PMF also revealed several energy minima and maxima in the constriction region, as well as in the NPA region. A more recent analysis of the PMF determined kinetics and conduction rates of glycerol through GlpF in good agreement with experimental data, and further explored the interesting asymmetry in the protein structure and the calculated PMF [206]. Interactive molecular dynamics simulations [207] with a pentatol substrate showed that very high force is needed to be applied particularly in the region of the selectivity filter, showing qualitative agreement with the steered MD studies of the natural substrate, glycerol, in GlpF.

5.2. Proton exclusion from aquaporins

From the earliest simulations, researchers have tried to understand how these membrane proteins allow water and glycerol to diffuse through while excluding protons, the movement of which would destroy the proton electrochemical gradient and starve cells to death. In simulations looking at water permeation, key structural features including the NPA motif, a constriction region (also termed ar/R), and the helix dipoles have all been implicated at different times as contributors to this specificity. Several models for proton exclusion have been proposed: (i) disruption of the hydrogen-bonded water file may prevent the formation of a perfect proton wire (a criteria of the Grotthus proton diffusion mechanism); (ii) electrostatic effects in the pore, particularly at the NPA motif, may present the major barrier for protons by restricting the rotational orientation of water in a manner that disrupts proton hopping [200]; and (iii) the electrostatic effects generated by charge–charge repulsion between positively charged elements in the pore and H_3O^+ ions block proton conduction through the channel [199]. Alternatively, proton exclusion may arise from the unfavorable effects of trying to pass a charged species through a narrow pore in a low dielectric medium [208]. Proton diffusion cannot be directly simulated with classical molecular dynamics since it involves quantum mechanical effects such as chemical bond formation and breakage and possibly proton tunnelling. Recent studies which have attempted to incorporate more physical descriptions of

proton transfer in the channel environment are presented here.

De Groot et al. [196] calculated a free energy profile for a proton moving through the channel, using a combination of molecular dynamics simulations and a description of proton diffusion termed Q-HOP [209]. The Q-HOP method uses regular molecular dynamics, but with periodic steps that describe the hopping of protons from hydronium (H_3O^+) ions to neutral water molecules, the acceptance of which depends on the relative orientations of the two interacting species and statistical mechanical principles. Regular molecular dynamics simulations that included hydronium (H_3O^+) and hydroxyl (OH^-) ions were also used to study normal diffusion of these species without considering bond dissociation. This study corroborated the findings of Jensen et al. [201] in that the NPA region was found to form the most significant barrier to proton conduction. This study used classical MD simulations where the electrostatic contributions in the NPA motifs and the helices of the re-entrant loop motifs were manipulated to illustrate that the electrostatic contribution of these protein features controlled the orientation of water dipoles in the pore. In the absence of the natural electrostatic environment, a regular water wire was formed (which could possibly conduct protons via the Grotthus mechanism). Similar results were observed in simulations of carbon nanotubes modeled with varying charge distributions that mimic the pore of AQP [210]. The dipole orientation of water molecules was observed to invert in these model biological channels as they do in the protein channel, as a result of the macrodipole exerted by the helices of the re-entrant loop motifs. In the protein simulations [201], the NPA motif was the strongest contributor to stopping proton hopping, because of the manner in which a water molecule is hydrogen-bonded between the two Asn sites of the NPA motifs. As observed through simulation, protons would be prevented from hopping past this site since this water molecule is fully saturated with hydrogen bonds.

Related work used the PM6 dissociable water model (described in a previous section of this review for gramicidin A) in a simulation of a single GlpF channel with water on either side [211]. This investigated the two steps of the Grotthus hop-and-turn mechanism by estimating the free energy for both of these steps. Direct simulation of proton hopping along the chain showed the existence of a significant electrostatic barrier in the centre. In addition, water on each side of the NPA motif is so strongly oriented that the turning step in the hop-and-turn mechanism is very unfavorable. It appears therefore that the electrostatic field in the channel prevents proton transport by restricting the orientation of water molecules and by presenting an electrostatic barrier to the movement of positively charged ions.

Another study used the MS-EVB2 [212] potential function to calculate the free energy barrier to explicit proton transfer in a single GlpF channel with water on each side of the channel and in the presence of an electric field [213]. The MS-EVB2 model explicitly describes the physics of proton transport and shuttling in aqueous protein environments. Their results showed two barriers to proton transfer, at the selectivity filter and the NPA motif. The largest barrier was seen at the NPA motif, which was thus concluded to be the main one to proton transfer. The smaller barrier at the selectivity filter may contribute to the exclusion of large solutes and ions.

In contrast to the aforementioned studies, a recent publication by Burykin and Warshel [208] proposed a mechanism for proton exclusion that depends only on the existence of a relatively hydrophobic channel, similar to what is seen in AQP1 and GlpF. The authors used MD simulations to generate configurations of a system consisting of a spherical water droplet, an AQP1 monomer and an array of carbon atoms to represent the low dielectric environment of the membrane. Configurations generated by MD were subjected to electrostatic energy calculations, and energy profiles for both hydronium ions and water molecules were calculated through the pore. Their analysis suggested that the NPA motif and dipole inversions investigated by other researchers [196,201] had an insignificant effect on proton exclusion. To illustrate this point, a similar calculation was conducted on a purely hydrophobic cylindrical pore, which gave results that were similar to those from the AQP1 pore.

While many of the studies mentioned above show qualitatively similar results, their quantitative results are quite different; to some extent, results are subject to the model applied. This topic will continue to be addressed in future work.

6. Ion channels

Ion channels were among the first membrane proteins to be studied by simulations, in particular gramicidin A. It is therefore not surprising that the major progress in structure determination of membrane proteins has spurred great interest in simulations of ion channels. Well over a dozen computational studies of the KcsA potassium channel have been published since its crystal structure was solved in 1998 [214], and many more studies on homology models of potassium channels as well as on the large conductance mechanosensitive channel (see below). More recent structures, including a higher-resolution KcsA structure [215,216], the structure of the MthK potassium channel in its open state [217], a chloride channel [218–221], the voltage-gated potassium channel KvAP [222–224] and the inward rectifier KirBAC [225], have also begun to be studied by simulations, both molecular dynamics and other methods. There are several reviews that cover a significant part of the literature, including a practically comprehensive review of work until about 2001 [158] and reviews focused on potassium channels [226–229].

Ion channels are an interesting category of membrane proteins for theoretical studies because of their (deceptively) simple function: transporting ions across membranes in a controlled manner, giving rise to conductance, selectivity and gating that distinguish the channels from each other. Cartoon models for these processes have been used for decades [230], but with increasing knowledge of the structures of ion channels and improved theories, more quantitative models are becoming possible. Examples where atomistic simulations form the basis for calculating current–voltage (*IV*) curves are now available for gramicidin A and KcsA. Calculations aimed at determining the molecular basis of selectivity are becoming increasingly sophisticated. And finally, simulations and models are now also being used to investigate conformational changes as well as more subtle changes in electrostatic fields that might be linked to gating. These vary from rather subtle proposed changes in chloride channels to very drastic rearrangements in mechanosensitive channels and to a somewhat smaller degree potassium channels.

Molecular dynamics simulations only provide part of the complete picture in these studies, but the combined approach of different theoretical methods with different amounts of detail is beginning to give interesting results. Below we review a number of recent studies on different channels. A detailed and/or comprehensive review is outside the scope of this paper.

6.1. Gramicidin A

Gramicidin A remains an important test bed for understanding the complex microscopic interactions that underlie ion permeation and selectivity and is also of special interest because of the direct effects interactions with lipids have on its function. The small size of the protein and the availability of several high-resolution structures allow extensive calculations. Theoretical studies on gramicidin A have been reviewed by several groups and many older reviews are available [158,231,232]. We focus on new studies.

Gramicidin A occurs in two conformations, called head-to-head and double helix. The ion channel form is almost universally assumed to be the head-to-head form. Desformyl-gramicidin is a modified version that is an excellent water channel. De Groot et al. [233] investigated the dynamics of desformyl-gramicidin double helix and head-to-head models in a lipid bilayer and found that the double helix is more stable for desformyl-gramicidin A, and also has a much higher water-conductance approaching that of aquaporins. The head-to-head structure of gramicidin A suggests that gating (opening) in gramicidin A consists of the two monomers joining across the membrane to form a functional channel, whereas closing is caused by the two monomers separating. This process has been investigated in detail by Miloshevsky and Jordan [234] using a semi-microscopic model that can be used to pinpoint specific interactions, e.g., hydrogen bonds, that determine the rate of gating.

There are now several high-resolution structures of gramicidin A, solved under different experimental conditions by different methods, that differ in some structural details. Allen et al. simulated two recent structures, one from solid state NMR [235] and from solution NMR in micelles [236]. These structures differ in side chain rotamers as well as in backbone structure. Extensive MD simulations (100 ns) have shown that both these structures are relevant, but exist in a dynamic equilibrium. They were able to calculate the relative population of the two states and also showed that relaxation of the structure has a significant effect on the size of the barrier for ion permeation. A ‘relaxed’ structure from MD simulations has a lower barrier for cation permeation and gives better agreement with the experimental conductance rates than calculations based on the high-resolution structure directly [237]. This somewhat alters the results of Allen et al. who compared the potential of mean force for cation permeation based on simulations of gramicidin A with different force fields. These simulations gave too high a barrier, which might therefore be related to properties of the structure used for these simulations [238]. The ability to obtain accurate potentials of mean force for ion permeation is critical to link atomistic simulations to macroscopic observables like *IV* curves. Allen et al. made this link between their improved gramicidin A structure and macroscopic properties by Brownian dynamics calculations based on potentials of mean force obtained from umbrella sampling calculations and several novel corrections to correct for the finite size of the simulation box and the underestimated dielectric constant of the lipid interior. Based on the resulting potentials of mean force, good agreement with experimental conductance data on gramicidin A was obtained [239].

Gramicidin A also has been an important test case for ion channel permeation theories. Without going into any detail, recent papers have shown that classical Poisson–Nernst–Planck and similar theories break down, essentially because bulk electrolyte behaviour is assumed in the narrow channel [240], but that they can be improved in different ways [241,242].

6.2. Hydrophobic nanotubes and other ‘toy’ channels

Hydrophobic nanotubes form a new class of model systems that has arisen in the last few years, partly driven by interest in nanotechnology but also by recent structural advances that have shown that many actual ion and water channels contain surprisingly hydrophobic stretches. Such hydrophobic pores have been observed in rhodopsin, aquaporins, the mechanosensitive channel MscL and most notably in the nicotinic acetylcholine receptor. Simple models of hydrophobic channels have been very useful to investigate the properties of water by molecular dynamics simulations. Progress in this areas has recently been reviewed by Beckstein et al. [119]. Cyclic peptides that aggregate to form nanotubes are another example of

artificial channels that show promise as designer channels. One example is a recent paper by Tarek et al. [243], who simulated a model of a channel formed by stacked cyclic peptides.

6.3. Mechanosensitive channels

Several species of mechanosensitive channels have been identified and the crystal structures of the large conductance mechanosensitive channel (MscL) from *M. tuberculosis* at 3.5 Å and the small conductance mechanosensitive channel (MscS) from *E. coli* at 3.9 Å have been solved [244]. Both these channels have intriguing properties. MscS is gated both by tension and voltage, and appears to have arginine residues exposed to the membrane that are important for voltage sensing [245]. This is particularly interesting in the context of voltage-gated sodium/calcium/potassium channels which contain highly conserved arginines [246]. MscL is sensitive to tension only. It has such a large conductance in the open state it must undergo very substantial conformational changes from the crystal structure, which appears to be closed. MscL is a pentameric protein consisting of two concentric rings of helices. The TM1 helices line the pore, and the TM2 helices form the outer ring. MscL also has a cytoplasmic C-terminal domain that is probably not involved in gating of the channel, but may act as a size-exclusion filter [247].

MscL has been the subject of a significant number of simulation and modeling studies aimed at understanding the gating mechanism, using the crystal structure or homology models of the *E. coli* MscL (Eco-MscL). The first simulations studied the crystal structure and several mutants to identify mobile and less mobile regions in the structure and to get hypotheses for further experimental studies [248,249]. The most interesting question is perhaps how the structure changes under the influence of membrane tension. Several hypotheses have been put forward, falling in two broad categories (Fig. 6). In the first, the TM1 and TM2 helices might form a larger 'barrel'. In this scenario, the TM2 helix might be the 'tension sensor' and undergo a significant conformational change that is eventually causing a change in TM1 as well to open the channel. In the second, the TM1 and TM2 rings of helices might move together in an "iris-like" motion that opens the channel, analogous to the lens of some cameras, while keeping the direct interactions between TM1 and TM2 helices the same. The net effect in both cases is a sharp increase in the pore radius. The first possibility seems to be suggested by MD simulations that apply a surface tension to the membrane or an explicit force on the protein directly [249–251]. The advantage of such simulations is that no preconceived notion of the mechanism is imposed, but a significant drawback is that such high surface tensions or forces are required to see structural changes on a nanosecond time scale that there is a considerable risk of simulation artefacts. In an interesting refinement of the idea of directly applying forces to a protein, Gullingsrud and Schulten [252] mimicked the effect of a surface tension by calculating the pressure distribution in a bilayer and applying a different tension to different parts of the protein, a model of *E. coli* MscL. The second mechanism, the iris mechanism, has been investigated by molecular modeling and extensive mutagenesis experiments [253,254]. The mutagenesis experiments are consistent with this mechanism. EPR experiments that measure the accessibility to hydrophilic and hydrophobic spin quenchers and the dynamics of every single residue in MscL also support the iris mechanism [255]. Finally, normal mode analyses of both the crystal structure and modeled intermediates suggest this mechanism [256]. It is interesting to note that a recent study based on cysteine cross-linking and molecular dynamics suggests that the cytoplasmic C-terminal domain does not open during gating

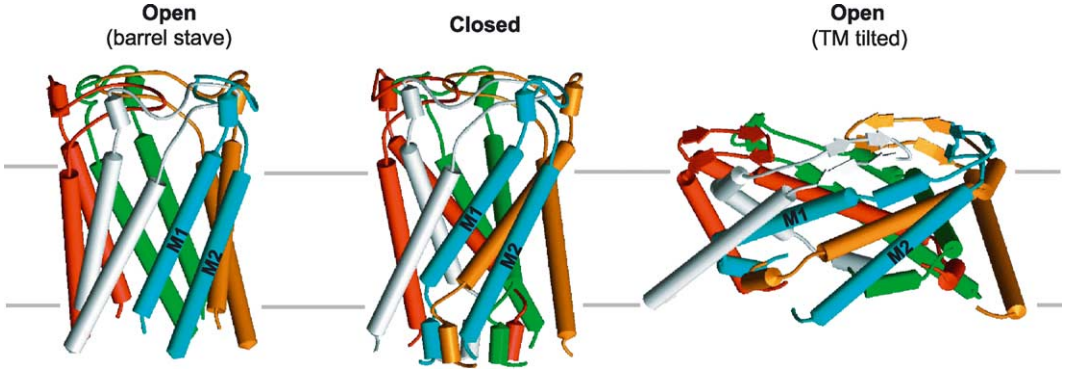

Fig. 6. Two proposed models for gating of the mechanosensitive ion channel MscL. The channel is a pentamer, and monomers are shown in different colors. A small cytoplasmic domain, composed of a bundle of helices, is not shown here. In the closed state, the channel is lined by M1 helices. The pore may open through a rearrangement process that results in all 10 helices (two per monomer) lining the channel (left), yielding a pore diameter of 16–18 Å. Alternatively, relatively rigid monomers may tilt significantly while approximately maintaining the relative orientations of helices M1 and M2 (right), resulting in dilation of the pore to around 30-Å diameter. The barrel stave model produces a pore that may be too small and is lined partially by hydrophobic residues from helix M2, whereas the TM-tilted model satisfies a number of experimental criteria and reproduces the predicted pore diameter. Figure reproduced with permission from review by Perozo and Rees [244]. See Sukharev et al. [254] and Betanzos et al. [253].

[247], which had previously been assumed. Eventually a crystal structure of MscL trapped in the open state, which would probably be a mutant that might be based on modelling, might help to explain the different results and to further hone the battery of computational and experimental methods used to obtain models of states that are not directly accessible by high-resolution structural methods.

6.4. Potassium channels

Potassium channels play diverse roles in cells, including electrical excitability, control of membrane potentials, volume, and release of insulin. They are characterized by their conductance, their selectivity, and a range of possible states that include open and closed, but often other states as well. Crystal structures have provided an unprecedented view of the molecular architecture of these channels but have also raised many questions. There have been a large number of simulation studies of potassium channels since the first structure was published in 1998. These studies include a dozen papers on simulations of KcsA, simulations of interactions of blockers with homology models of Shaker, studies on homology models of inward rectifier channels, models of the open state of a potassium channel based on the closed KcsA structure and more recently also on the open MthK channel, studies on the molecular basis of selectivity between different cations, as well as interesting hierarchical approaches aimed at linking the atomistic KcsA structure to the observed current–voltage (*IV*) curves. Many of these studies have been reviewed multiple times in the past year [1,158,227,229] and we focus on very recent papers.

6.4.1. Permeation and selectivity

The overall shape of KcsA resembles a truncated cone with a central pore running down the centre. The wider end of the cone corresponds to the extracellular mouth of the channel. The transbilayer pore is formed by a bundle of eight TM helices, four M1 and four M2 helices. The selectivity filter with the K channel signature motif TVGYG is located near the extracellular mouth of the channel. This filter contains distinct ion binding sites that are well resolved in the crystal structures. The first simulation studies of KcsA focused on microscopic motions of ions in the selectivity filter. A main result was the confirmation that ions and water indeed move as a single file in the selectivity filter and that the filter deforms significantly during the translocation process. Simulations of several nanoseconds are not enough to get any statistics on ions leaving or entering the channel or filter, although simulations by several groups have observed individual events.

One of the most recent and quite elaborate studies on the behaviour of the selectivity filter and ions in the selectivity filter is a paper by Domene and Sansom [215], in which different cations (Na^+, K^+, Rb^+, Cs^+) were simulated in the high-resolution crystal structure of KcsA. This work can be compared to similar simulations on Na^+ and K^+ in the selectivity filter based on the 1998 crystal structure [257]. These older simulations missed several refinements, such as the inclusion of water molecules behind the selectivity filter. Nonetheless, in both simulations significant flexibility of the filter was observed, as well as concerted motions of ions and water. In particular, pronounced distortions of the filter occur when no ions are present, which is also found from crystallographic studies at low salt concentration [258]. The two most readily permeant ions, K^+ and Rb^+, are similar in their interactions with the selectivity filter, while Na^+ ions tend to distort the filter by binding to a ring of four carbonyl oxygens (Fig. 7).

The larger Cs^+ ions result in a small degree of expansion of the filter relative to the X-ray structure and show some tendency to bind within the gate region of the channel, near the cavity.

Although simulations of ions depend critically on ion–water and ion–protein parameters, recent results of MD simulations seem consistent with experimental data as well as internally. Relative stabilities of these different ions in ion channels can be calculated from free energy perturbation or similar approaches [158], but obtaining sufficient sampling in such simulations is challenging, and it is very

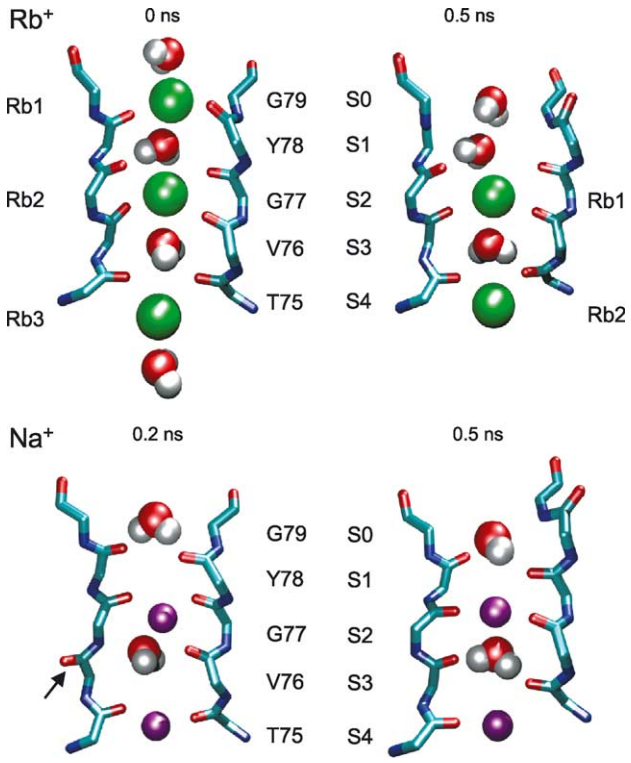

Fig. 7. The selectivity filter of KcsA with Rb^+ and Na^+ ions. Residues contributing their backbone carboxyl groups to the selectivity filter are G79, Y78, G77, V76 and T75. Ion occupancy sites are labelled S0 through S4. The much smaller Na^+ ions (lower panel) are thought to be less stabilized in the selectivity filter than the larger Rb^+ ions, which are conducted similarly to potassium (upper panel). Disruption of the backbone resulting from lost electrostatic interactions is apparent in the presence of Na^+ (black arrow, lower panel). Reproduced with permission from Domene and Sansom [215].

important to have accurate interaction potentials. Roux and Bernèche [259] have pointed out that even in the case of sodium and potassium, the two most commonly used ions, the interaction energies between these ions, water, and peptide backbone are very difficult to represent accurately. A similar critical study of cesium and rubidium is urgently needed to better understand the maximum accuracy that can be obtained by MD simulations with current methods. The relative stabilities of different cations in the filter depend on the relative difference in solvation free energy in water and inside the channel, which is a small difference between large numbers. These numbers too are challenging to reproduce accurately, and there is a surprising additional problem (because it seems such a fundamental property): experimental data for hydration free energies of single ions is difficult to obtain with accuracy, essentially because there are always counter-ions present in experiments [260].

Microscopic simulations on a nanosecond time scale are several orders of magnitude in simulation time away from direct calculation of currents. Several recent papers have however used microscopic calculations to calculate the potential of mean force, the effective energy surface that ions move on, for ions in KcsA, either in full atomistic detail [261] or in simplified representations [262]. Berneche and Roux [263] used their multi-dimensional potential of mean force as potential for Brownian dynamics simulations to calculate current–voltage curves directly, with surprisingly accurate results. Burykin et al. [262] used their simplified representation of KcsA to investigate the relative contributions of a range of structural elements in KcsA and the environment to calculated conductance values. This illustrates the power of semi-microscopic models with less detail than atomistic MD to investigate contributing factors to permeation energetics in more detail. A very interesting recent example applied to KcsA is the work of Garofoli and Jordan [264], who investigated different ions in the selectivity filter.

6.4.2. Conformational changes in gating

Molecular dynamics simulations and modeling would seem ideal approaches to investigate the range of conformations an ion channel can adopt, given one known conformation from a crystal structure. The original structure of KcsA appears to be a closed state, and several groups have built models of what the open state might look like [265–267], using different procedures to displace the intracellular gate formed by the pore-lining helices (Fig. 8) [268].

Experimental support for conformational changes came from EPR measurements [269] and from accessibility studies that show which part of the pore lining helices is accessible from the intracellular side in the open state [270]. An elegant study of the classical phenomenon of N-type inactivation in a voltage-gated potassium channel also suggests the intracellular side of the channel must be able to open quite substantially compared to KcsA [271]. This was confirmed by the crystal structure of MthK, a calcium-gated channel that was crystallized in the presence of calcium, in an open structure [272]. The conformational changes compared to the closed structures of KirBAC [225] and KcsA [214] are substantial. Although they are larger than most predictions by simulation, several of the simulated/modelled structures are quite reasonable. This gives some confidence that simulation and simulation-based models will be useful in investigating a range of states of potassium channels, where it seems unlikely that they can all be trapped in crystal structures.

A more extreme example of conformational changes is presented by the crystal structure of the voltage-gated potassium channel KvAP [222] and models of Shaker [273]. There are now two major conflicting views of conformational changes associated with voltage-gating in a controversy that is outside the scope of this paper [274], but it is certain there will be a host of new simulation and modeling studies based on both the existing crystal structures and the large body of other experimental data on voltage gated channels, in particular Shaker. One

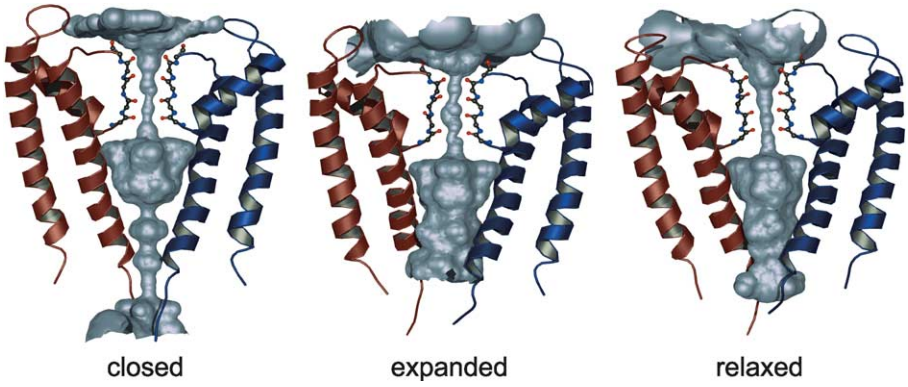

Fig. 8. Models for opening of the KcsA potassium channel. The expanded state was generated from the relaxed crystal structure (closed) with steered MD (in a membrane), by expanding a van der Waals sphere (or repulsive balloon) in the lower portion of the pore. The sphere was invisible to water, allowing it to fill the cavity during this process. The relaxed state was generated from the expanded state by freely simulating for an additional 10 ns. The profile of the pore is represented as grey density, and only two of the four monomers are shown (for clarity). Reproduced with permission from Biggin and Sansom [265].

example of a simulation of KvAP is a simulation by Monticelli et al. in which one proposed gating mechanism is 'tested' in a simulation by forcing the voltage paddle (S3–S4 helices) from the KvAP crystal structure to traverse the membrane, as proposed by Jiang et al. [224]. These simulations showed that the pore domain itself appears rather insensitive to changes in the S1–S4 domain, even under nonequilibrium conditions. Moving the paddles through the membranes created substantial water defects.

6.4.3. Homology models and potassium channel–toxin interactions

All solved crystal structures of potassium channels are bacterial, but there is great interest in eukaryotic channels. Because potassium channels are fairly conserved, certainly within major families like voltage-gated channels or inward rectifiers, homology modeling of eukaryotic channels is a useful way of assisting the interpretation of experiments and to help design new experiments. Such models typically use homology to KcsA, and now also MthK, KirBAC and KvAP, in addition to experimental distance restraints obtained from a range of techniques. Examples where such models were combined with molecular dynamics simulation are recent models of the inward rectifying channel Kir6.1 [275], of Shaker [276] to investigate interactions with agitoxin, and of Kv1.5 [277] to investigate interactions with drugs.

7. Computer simulation of ATPases

Several classes of ATPases facilitate transport across membranes [278], including F-type proton pumps and ABC transporters. F_1F_0 ATP synthase has been most extensively studied but several types of computer simulation have also been used to study recent structures of the ABC transporters. These serve as a good illustration of the challenges involved in venturing into a newly evolving area with substantial biochemical data but little detailed structural information.

7.1. ABC transporters

ABC-type transporters are one of the largest superfamilies of proteins [279] and play key roles of biomedical interest, including multidrug resistance in cancer cells and bacteria and in genetic diseases such as cystic fibrosis. They are found in both eukaryotic and prokaryotic systems and are easily recognizable by the characteristic LSGGQ signature motif of their ATPase domain. In spite of their significance, relatively little is known with certainty about the mechanism by which they use the well-conserved ATP binding cassette subunit to execute a wide variety of functions, including transport, ion conduction, receptor-mediated signalling, and DNA repair in related proteins.

Before the availability of crystal structures, computational studies of ABC transporters were focused mainly on structure prediction based on homology to other ATPases like F_1-ATPase and recA [280]. Molecular dynamics simulations aimed at elucidating the functional mechanics of ABC transporters are currently still sparse in the literature (Fig. 9). The first crystal structure of an ABC-transporter nucleotide binding domain (NBD) was reported in 1998 [281]. Several structures of nucleotide binding domains have been reported since but the major breakthrough came with the publication of the first crystal structure of a (nearly) complete transporter, composed of two transmembrane units and two NBDs in 2001 [282]. In this structure of the lipid A transporter MsbA from *E. coli*, the TMDs are closely associated on the periplasmic end of the membrane but the NBDs are 50 Å apart. The nucleotide-binding pockets face away from the dimer interface and are thus exposed to the solvent. Other high-resolution structures of assembled ABC transporters that have recently been reported are those of *E. coli* BtuCD and *Vibrio cholera* MsbA [283,284]. Although these rapid advances in structure determination have answered important questions about the fold and topology

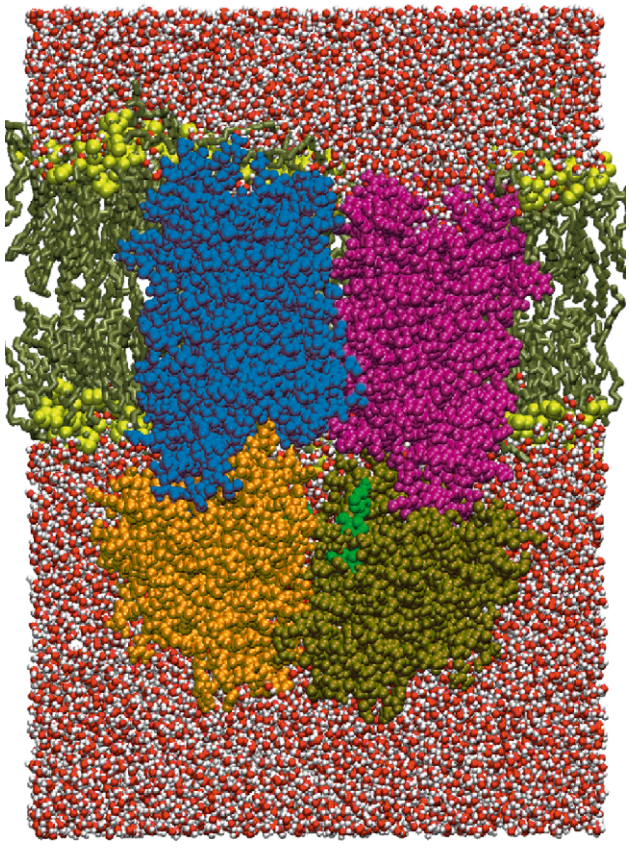

Fig. 9. A simulation box containing BtuCD in a POPE lipid bilayer (yellow head groups with brown tails) and solvated in a box of water molecules (red and white). The transmembrane domains, through which substrate is transported into the cytoplasm, are highlighted in blue and purple. The nucleotide binding domains that hydrolyze ATP are shown in orange and ochre. Two ATP molecules (not solved in the crystal structure) are docked into their respective catalytic sites to investigate the hypothesis that ATP binding represents the power stroke of the catalytic mechanism. One of the ATP molecules is visible in green.

of ABC transporters, the widely different conformations adopted by the NBDs have raised several key questions about the transport mechanism. Unlike in *E. coli* MsbA, the NBDs of *V. cholera* MsbA and *E. coli* BtuCD are in close opposition and face each other in the manner earlier proposed by Jones and George and subsequently reported for Rad50, an ABC protein involved in DNA repair [285,286]. This is in spite of the fact that all three structures did not have nucleotide bound at their catalytic sites. It is also intriguing that the conformational orientation of the NBDs of *V. cholera* MsbA and BtuCD are close but not particularly similar. The argument has been made that these differences are due to crystal packing forces in the structures of MsbA. The opposing view is that they may be indicative of the NBD's natural ability to sample a large conformational space during the catalytic cycle [283]. Computer simulation studies may help to shed more light in this area.

7.1.1. Structural modelling

The crystal structure of the NBD of HisP suggested a dimerization scheme in which the ATP binding site faced away from the "back-to-back" dimer interface, exposing the nucleotide to solvent. This was in contrast to other ATPases in which the nucleotides are buried. In an attempt to resolve this disparity, Jones and George [286] used computational methods to derive a new dimerization model in which both nucleotides are buried. Based on sequence alignment and mutational analysis results, they used the high-resolution structure of HisP and other nucleotide-binding proteins to propose a "head-to-tail" dimer in which each nucleotide is sandwiched between the LSGGQ signature motif of one subunit and the conserved nucleotide-binding (or Walker A) motif of the opposing subunit. This model was also consistent with cooperativity in ATP hydrolysis and the observed stringent requisite of two NBDs in each transporter. This model has since been confirmed by crystal structures of Rad50, MalK, and MJ0796 [285,287,288].

Other studies have used recently published crystal structures as templates to model medically relevant ABC transporters such as P-glycoprotein and MRP1/ABCC1 [289–291]. The first reported crystal structure of a "complete" ABC-transporter, MsbA from *E. coli* (EC-MsbA), was resolved at 4.5-Å resolution. This structure revealed only the C-α polypeptide trace of the protein, and coordinates for a significant part of the NBD consisting of 78 residues including the conserved ATP binding Walker A motif could also not be determined due to disorder. Thus, in spite of its reasonably good sequence homology to medically relevant human ABC transporters, the structure of EC-MsbA, as published, is of insufficient resolution to be used as a dependable template for homology modeling or as a starting structure for molecular dynamics computer simulation studies. An attempt was made to complete the EC-MsbA structure by modeling missing atoms [292]. Starting from the C-α polypeptide trace, the backbone and side chain atoms were generated, and the structure of the missing part of the NBD was modeled based on homology with known high-resolution structures of the NBDs of other ABC transporters. MD simulations were subsequently used to test the stability of the model. While the modeled monomer was conformationally stable when subjected to MD simulation, the dimer as assembled in the crystal structure was not. This, in conjunction with other experimental biochemical data, was taken as an indication that the crystal structure may not represent a physiologically relevant dimer conformation.

Stenham et al. reoriented the TMDs of EC-MsbA with respect to the NBDs in order to transform the "back-to-back" dimer into a "head-to-tail" model. They thus obtained a suitable template for modeling P-glycoprotein, yielding a structure that satisfied cysteine cross-linking data, information from electron microscopy, and structural information from isolated nucleotide-binding domains [291]. More recently, MRP1 has been homology modeled following a similar protocol using the aforementioned P-glycoprotein model and the *V. cholera* MsbA crystal structure as templates for the TMD, and the MJ0796 dimer as a template for the NBDs [289].

7.1.2. MD simulations

Important details of the mechanism that couples conformational changes caused by ATP binding, hydrolysis, and ADP+Pi release in the cytoplasmic domain to the translocation of substrates through the transmembrane domain remain unknown. These and other aspects of the detailed mechanism of ABC transporters, which are challenging to study experimentally, are well suited for study by MD simulations. The atomic level of detail accessible can provide useful insights needed to relate the 3D structures of ABC transporters to their functional mechanism.

Few straightforward MD simulation aimed at elucidating the functional dynamics of ABC transporters have been reported [292,293]. The 390-ps simulation study of the isolated nucleotide-binding domain of HisP identified hinge and switch regions possibly involved in conformational transitions within the nucleotide-binding domain. Comparison of crystal structures led to the suggestion that a conserved glutamine-containing loop (the Q-loop) could adopt either an extended or a coiled conformation. This is believed to result in movement of the conserved glutamine (Q-100) of the Q-loop in and out of the catalytic site [285]. Based on their simulation study, Jones and George proposed that the peptide bond between F99 and Q100 as well as residues 4 and 5 immediately C-terminal to the Q-loop could act as hinge points for this motion. They further proposed that this loop might be involved in subunit contact with the TMDs.

Simulation studies of the full transporter comprising the TMDs and the NBDs are yet to be reported. Preliminary results from our lab towards this end show that important mechanistic insights can be drawn from MD simulation of

BtuCD in a realistic lipid bilayer (Fig. 9). The protein remains stable during 15-ns simulations but undergoes conformational changes propelled by the introduction of nucleotides at the catalytic sites (Oloo and Tieleman, unpublished).

7.2. F_1F_0 ATP synthase

The molecular motor protein F_1F_0 ATP synthase is one of the most abundant proteins in living systems. It performs the crucial role of synthesizing ATP, the universal energy currency of the cell, from ADP and Pi [294,295]. ATP synthase is particularly attractive to computational biologists for several reasons. First, there exists a large amount of experimental data relating to stoichiometry, substrate binding affinities, thermodynamics, and kinetics, as well as cross-linking and mutational studies. Due to its unique mechanism, ATP synthase has been described as an enzyme that functions very much like a man-made motor [296]. The protein has three catalytic sites whose nucleotide affinities change as the motor rotates (Fig. 10). Rotation of the motor is reversible so that it can synthesize or hydrolyze ATP. In the ATP hydrolysis direction, one revolution of the motor requires about three times the free energy of ATP hydrolysis

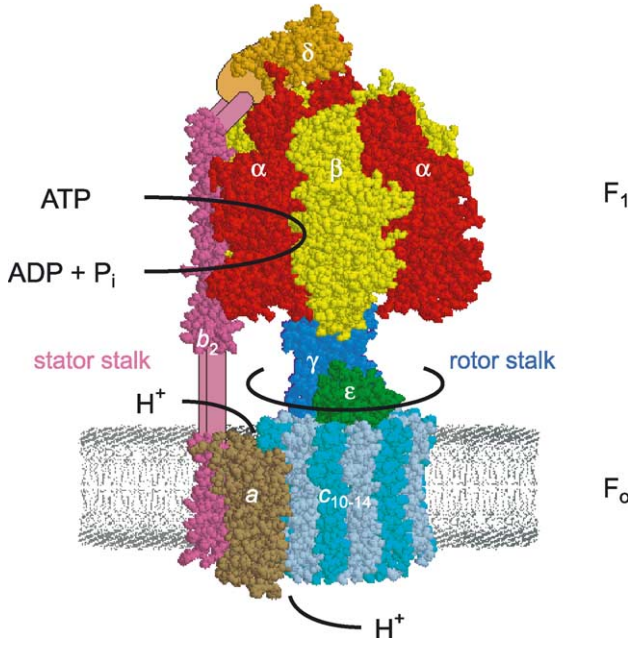

Fig. 10. F_1F_0 ATP synthase is a large protein consisting of a proton-translocating transmembrane domain F_0 and a cytoplasmic domain F_1. F_0 is composed of subunits a, b_2, and c_{10-14} (a ring consisting of 10 to 14 identical subunits) while F_1 is made up of subunits $(\alpha\beta)_3$, γ, δ and ε. The γ/ε portion is a central stalk that links the cores of F_0 and F_1 by making strong contacts with the c ring at the membrane end and fitting inside the three α and β subunits arranged around it in an alternating fashion at the cytoplasmic end. Downhill proton transport through the F_0 domain is believed to physically drive the rotation of the central stalk (along with the c subunit) counter to the $(\alpha\beta)_3$ portion thereby altering the conformation and nucleotide binding affinity at the three β catalytic sites. Reproduced with permission from Weber and Senior [295].

implying ~100% mechanical efficiency [297]. The maximal rate of ATP hydrolysis is ~300/s [296].

Structural studies have been aided by the fact that F_1 can be reversibly separated from F_0 and crystallized separately. F_1 separated from F_0 can still hydrolyze ATP. Currently, most of the structure of ATP synthase is known in atomic detail except the a-subunit, the C-terminal end of the δ subunit and portions of the b-subunit (Refs. [15–21 in 295]). The F_1 domain is thus much better studied by computer simulation than the F_0 domain. Three different conformations of the beta subunit observed in the crystal structure of mitochondrial F_1-ATPase were designated as β_{TP}, β_{DP} and β_E [298]. Each catalytic binding site is expected to go through all three states in sequence during the hydrolysis or synthesis cycle. Indeed, the F_1 domain's motor action has been demonstrated experimentally at sub-millisecond resolution by tethering an actin filament or bead to the exposed part of the central stalk. Under a microscope, the actin filament was observed to rotate anticlockwise (viewed from the membrane) in 120° steps during ATP hydrolysis [299].

The focus of computer simulation studies has been to derive a mechanistic scheme that correlates well with existing experimental data. Computer simulation methods that have been applied to ATP synthase include interpolation, equilibrium molecular dynamics, biased molecular dynamics, targeted molecular dynamics, free energy simulations and QM/MM. Samples of studies exploiting each technique are discussed below to illustrate the kind of insights that can be gained from them.

7.3. The F_1 sector

7.3.1. Interpolation techniques

Interpolation helps to cover long time scales that are inaccessible to straightforward simulation. In one of the early modeling studies, Wang and Oster [300] created an animation of the complete motion of F_1 through a hydrolysis cycle. This was done by structure interpolation between 0° and 120° in a cylindrical coordinate system. From a study of the derived pathway, they concluded that the rotation of the γ stalk is tightly coupled to structural rearrangement in the binding pockets. They further concluded that the F_1 domain converts the free energy of ATP binding into elastic strain in its β subunits. The subsequent release of this strain is harnessed to create rotary torque on the γ shaft.

In a recent study based on the interpolation technique combined with computer simulations of equidistant interpolated structures, Antes et al. [301] studied the unbinding of ATP from the catalytic site. In this work, only atoms distant from the nucleotide-binding site were interpolated. Atoms close to the binding sites were allowed to equilibrate during the MD simulation process. The unbinding process was shown to involve the sequential weakening and ultimate breakage of specific hydrogen bonds between ATP and the α and β subunits.

7.3.2. MD simulations

Equilibrium MD simulations (without any bias, steering or acceleration) of ATP synthase are not common considering that events of interest like ATP binding or release occur on the millisecond time scale but the large size of the protein limits simulation to the nanosecond. A few straightforward simulation studies have, however, been reported. Böckmann and Grubmüller [302,303] attempted to trace the origins of a fast nucleotide-independent closure of the β_E binding pocket they had previously reported in a biased molecular dynamics study. They performed a straightforward MD simulation of the isolated β subunit. Even when isolated, the β_E subunit underwent a spontaneous closure similar in motion and kinetics to those observed in the simulation of the full transporter. This spontaneous closure therefore appears to be caused by elastic strain within the β subunit rather than interaction with the neighbouring α and γ subunits.

7.3.3. Biased molecular dynamics

Several studies have been centred on the application of a biasing force to cause 120° rotations of the central stalk. The drawback with this method is that key relaxation events may be missed when a process that occurs in the millisecond time scale in nature is forced to occur on the nanosecond time scale accessible to protein MD simulations. Biased molecular dynamics simulations thus do not yield a full transition path. However, useful mechanistic information can still be derived from such studies. Böckmann and Grubmüller imitated the pH-gradient-driven rotation of the central stalk by performing a molecular dynamics simulation during which the γ subunit stalk was forcibly rotated 120° in the ATP synthesis direction over 7 ns [302]. They were able to determine that binding affinity for ATP at the β_{TP} catalytic site was diminished as a result of conformational changes induced by the rotation. A sequential withdrawal of three arginine residues leading to the rupture of hydrogen bonds with ATP was seen. This was considered to correspond with the ATP release step of the ATP synthesis cycle. The empty binding pocket, β_E, also underwent fast spontaneous closure independent of nucleotide occupancy.

7.3.4. Targeted molecular dynamics

In targeted molecular dynamics simulations [304], the entire system is constrained to pursue a low energy pathway between two end states. This yields a full path from one end point to the other. In a study based primarily on targeted MD complemented with biased MD, Ma et al. [305] investigated the dynamics of structural transitions accompanying the rotation of γ subunit in the direction of ATP synthesis and the order in which they occur. This simulation study revealed that the counter-rotatory motion is guided over the 120° span by a track of positively charged Arg and Lys residues on the γ subunit interacting with negatively charged Glu and Asp side chains on the β subunit.

7.3.5. Free energy simulations

Three sets of similar crystal structures of bovine mitochondrial F_1-ATPase have revealed different nucleotide bound states at the three catalytic sites designated β_{TP}, β_{DP} and β_E. Experimental measurements in solution have also shown the existence of a tight, a loose and a weak binding site for ATP. There is general agreement that the β_E site is the weak-binding site. Using free energy difference simulations for the hydrolysis reaction in each site, Yang et al. [306] were able to identify the β_{TP} and β_{DP} catalytic sites of mitochondrial F_1 as the tight and lose binding sites, respectively, for ATP. Their results further showed that despite their similarity in structure, binding free energies at the β_{TP} and β_{DP} catalytic sites are modulated by differences in the contributions of a number of mainly charged residues to the interaction with nucleotides.

One of the difficulties in the experimental study of F_1F_0 ATP synthase, ABC transporters and other motor proteins is to accurately map known X-ray structures to different states adopted by the nucleotide-binding subunits during the catalytic cycle. Štrajbl et al. [307] attempted to do this for F_1 ATP synthase by adopting a computer-aided strategy based on linear response approximation (LRA) and evaluation of the free energies of transition between conformational states. They also calculated free energies of transferring ligands from water to different binding sites of F_1-ATPase in their different conformational states, i.e., β_E, β_{TP}, and β_{DP}. Finally, they used empirical valence bond analyses to calculate the free energy profile of ATP synthesis in each conformational state. Their results show that electrostatic free energies rather than steric energies can describe most of the energetics of the system during the catalytic mechanism of F_1 ATP synthase. Change from the β_{DP} to the β_{TP} conformation causes stabilization of the ATP state relative to the ADP state by shifting electrostatic potential away from the β-phosphate towards the γ-phosphate. Electrostatic repulsion between ADP and P_i was found to contribute significantly to the energy difference between ATP and ADP+P_i. They conclude that changes in charges of ligands during the catalytic cycle cause protein reorganization and that the effect of the rotation of the gamma stalk is mainly electrostatic.

7.3.6. QM/MM

Processes involving the breaking of chemical bonds are not amenable to molecular dynamics simulation. A quantum mechanical (QM) treatment is needed. However, QM is computationally expensive and currently limited to a few hundred atoms. The QM/MM method is a technique used to get around this hurdle. The reactive centre and its immediate surroundings are modeled in electronic detail using a quantum mechanical approach while the rest of the system is treated classically to atomic detail using molecular dynamics. Dittrich et al. have performed a QM/MM study of the ATP hydrolysis process in the β_{TP} site of F_1. They find that the ATP hydrolysis reaction in this site is strongly

endothermic suggesting that the conformation at the β_{TP} site inherently discourages ATP hydrolysis. They also identify the reaction path with minimum potential energy barrier as one in which two water molecules are involved in the nucleophilic attack of gamma phosphate compared to the conventional attack by a single water molecule [308].

7.4. The F_0 sector

Progress in computer modeling studies of the F_0 sector has lagged behind studies of the F_1 part due to the lack of a crystal structure that includes both the a- and c-subunits. Each monomer of the c-subunit is an α-helical hairpin composed of an inner transmembrane helix (TMH) and an outer TMH that interfaces with the a-subunit (Fig. 10). Aksimentiev et al. [309] have recently reported the use of a modelled structure to investigate the mechanism of torque generation in the F_0 domain. In this study, biased molecular dynamics simulations and mathematical modeling were employed to characterize changes at the interface between the a- and c-subunits. To imitate motion during the catalytic mechanism, forced rotation of an outer TMH about its axis was performed with the backbone atoms of its corresponding inner TMH restrained. Similarly, the entire C_{10} oligomeric unit was forced to rotate relative to the a-subunit. Based on their results, the authors conclude that rotation of the outer TMH of the c-subunit switches the accessibility of the proton-binding site's Asp-61 from the periplasm to the cytoplasm. They therefore propose a proton transport mechanism in which the rotation of the entire c-subunit as well as of individual TMHs in the c- and a-subunit are coupled to the protonation state of Asp-61 located in the middle of each outer TMH. A stochastic model that simplifies the dynamics of the F_0 domain to a few essential degrees of freedom was developed to assess this mechanism. Since computational studies based on modelled structures are particularly susceptible to errors inherent to the starting conformation, additional structural data to verify the correctness of the interfacial alignment of the a-subunit relative to the c-subunit would be important in validating the proposed proton translocation mechanism.

8. Outer membrane proteins

β-barrel membrane proteins are unique to the outer membranes of mitochondria, chloroplasts, and gram-negative bacteria. The bacterial proteins, which range in size from 8 to 22 β-stranded barrels, perform a variety of functions, from enzymatic lipid cleavage to nutrient uptake functions to iron transport [310,311]. A relatively large number of crystal structures are available (for example [312]) so that combined with lipid models of LPS and other lipids, it is becoming feasible to construct a computational model in atomic detail of the entire bacterial outer membrane [1]. In this section, recent MD simulations of OmpF, OmpA, OMPLA, and FhuA will be reviewed.

8.1. OmpF

The porin OmpF could be considered the prototypical outer membrane protein and was also the first to be simulated in an explicit lipid environment [313]. Over a 1-ns simulation, Tieleman and Berendsen observed that water in the pore was highly organized and behaved in a significantly different manner than bulk water. The lipid–protein interactions of OmpF in a POPE bilayer were analyzed in detail [314], and it was observed that the presence of the membrane protein affected numerous bilayer properties including lipid order parameters and bilayer thickness. Robertson and Tieleman [315] performed further studies on the potential role of the L3 loop in the constriction site for OmpF's voltage sensitivity by simulating trimeric OmpF in a DMPC bilayer with applied electric fields of different strength. Some voltage-dependent effects were observed but the molecular basis of 'voltage gating' in OmpF remains unclear, despite recent experimental progress [316]. The diffusion of ions through OmpF has also been studied [317]. Simulations of OmpF in a DMPC bilayer, at 1 M KCl concentration over 5 ns allowed for a direct study of ion distribution in the pores. The authors observed that K^+ had a higher occupation propensity than Cl^- in the pore, as would be expected of this cation selective pore. Simulations also demonstrated that K^+ could move through the pore independently, but Cl^- ions only permeated through the pore in the presence of K^+ counter-ions. The screw-like pathways followed by the cation and anion appeared to be distinct along the pore axis. Interestingly, the ion distribution calculated from the equilibrium MD simulation was quite similar to those obtained from Brownian dynamics and Poisson–Nernst–Planck theory, two progressively more simplified theories [317]. Robertson and Tieleman [318] studied diffusion of polar molecules, alanine and methylglucose, through the OmpF trimer using nonequilibrium steered molecular dynamics. These dipolar molecules align strongly in the eyelet region's electric field.

8.2. OmpA

OmpA is a small outer membrane protein expressed at high levels in monomeric form. It has an N-terminal eight-stranded beta-barrel domain (171 residues), which has been crystallized at 1.65-Å [319] and 2.5-Å [320] resolution. The C-terminal domain has unknown topology, although a crystal structure has recently been obtained for a homologous domain from the protein RmpM [321]. This periplasmic domain is believed to function as an anchor of peptidoglycan to the outer membrane [310,312,322]. The functional features of OmpA are hotly debated. Some experimental studies have observed ion channel activity while the crystal structure shows OmpA to be an inverted

micelle, with a hydrophobic exterior and polar side chains in the centre of the protein that could essentially block any possible transport [311,322]. Water molecules have been crystallized in the polar interior of OmpA, but are distributed as three distinct groups; a continuous water file or pore is not observed. In MD simulations of OmpA, Bond and et al. [323] observed that while water molecules were present in the region of the "polar ring" of conserved residues (Lys12, Glu140, and Arg96) at the extracellular face and past the "periplasmic cover", full permeation events were blocked by the "gate" formed at the centre of the protein via a salt bridge between the conserved residues Arg138 and Glu52 (Fig. 11) [323]. By manually isomerizing the Arg138 residue, another suitable salt-bridge partner, Glu128, was identified. With the gating salt-bridge broken, complete permeation events of water were observed. The new model showed an overall increase in the pore radius, with an estimated conductance that was similar to experimental values, suggesting isomerization of the Arg138 side chain as a potential gating mechanism of OmpA. In another MD simulation study of OmpA, Bond and Sansom [324] compared protein behaviour in a DMPC bilayer and a dodecylphosphocholine (DPC) micelle. In the OmpA/micelle simulation, RMSD and RMSF analyses showed increased mobility of the structural features of the protein. This resulted in full permeation of water through the protein in the micelle environment, without any manual modification of residues in the protein interior. The increased mobility of the protein in the micelle environment allowed Arg138 of the gating salt bridge to explore different side chain torsion angles, resulting in a mean increase in pore diameter. These results illustrate how sensitive proteins are to the lipid environment, and suggest that reconstituting isolated OmpA into micelles and then into bilayers may affect the dynamic features of the protein.

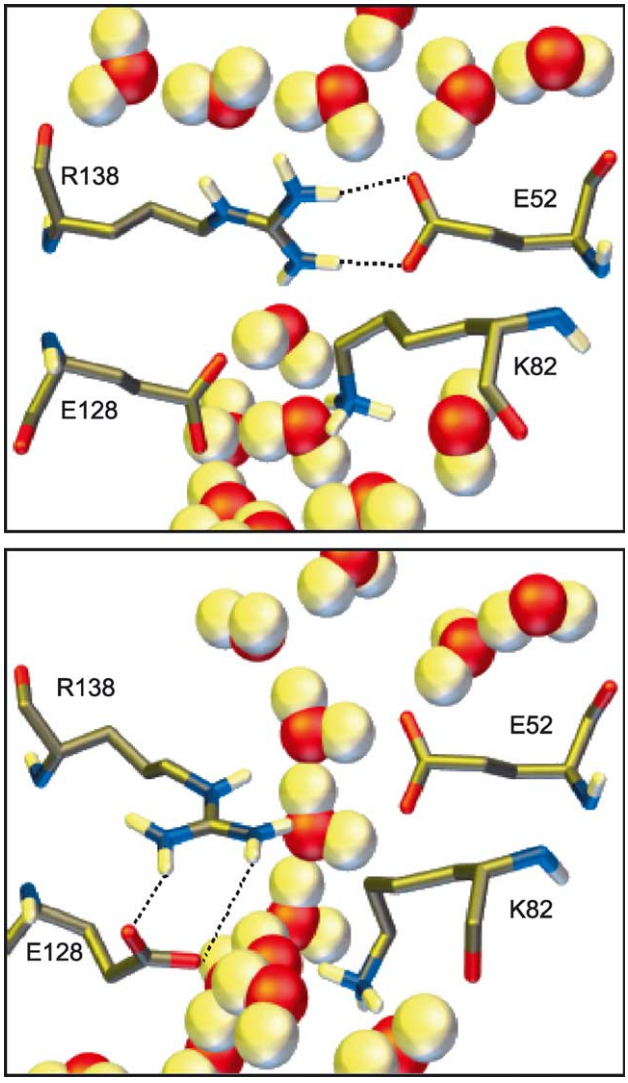

Fig. 11. A proposed gating mechanism for OmpA is shown in which a key arginine (R138) alternates salt-bridge interactions between two glutamine side-chains (E52 and E128). In simulations of the two states, it is apparent that water is blocked in one case (top panel) and can flow through the pore in the other (bottom panel). Reproduced with permission from Bond et al. [323].

8.3. OMPLA

OMPLA is a membrane-bound calcium-dependent enzyme that hydrolyzes a variety of phospholipids and diglycerides [325]. It is located in the outer membrane as a 12-stranded β-barrel monomer, but dimerizes to perform its enzymatic function. Topologically, each OMPLA monomer has a "flat" and a "convex" side. The flat sides of two OMPLA molecules face each other in the dimer in the crystal structure. The topologies of OMPLA in monomeric and dimeric forms are nearly identical, which gives little insight as to why the protein needs to dimerize to perform its enzymatic function. Baaden et al., in simulations of both monomeric and dimeric OMPLA, explored dynamic differences that might be related to enzyme function [326]. The simulations showed a stabilizing effect of dimer formation, in particular on the proposed enzymatic active site. As a (Ca^{2+} free) monomer, the active site was quite flexible, but in the dimer forms studied, the Ca^{2+} ion stabilizes a network of hydrogen bonds with three water molecules that in turn stabilizes the active site. Further to that, the authors observed a collapse of the binding pocket and reduced solvent accessible surface area in the substrate free dimer compared to the dimer with both Ca^{2+} and substrate bound. This observation may explain the experimentally observed inactivity of some OMPLA dimers [326].

8.4. FhuA

FhuA is a siderophore receptor and transporter through the outer membrane, related to FecA, FepA and BtuB [312]. FhuA is one of the largest monomeric β-barrel MPs, at 22 β-strands. The central pore of the barrel is

plugged by a potentially removable N-terminal polypeptide domain, the "plug", although it remains unclear whether this plug can move, and how substrates are moved through outer membrane receptors [327–330]. Some change in the conformation or position of the plug domain must occur to allow translocation; this is proposed to be mediated by TonB and associated proteins. Simulations of FhuA with and without bound ferrichrome were performed to study barrel–plug and barrel–siderophore interactions [331]. Over the 10-ns simulation, it was observed that the plug domain is stabilized by many hydrogen bonds (on the order of 50), in both the ferrichrome-bound and unbound states. It does not seem likely that the plug domain could rearrange to such an extent as to allow the ferrichrome to simply diffuse across the system. The authors suggest applying a steered MD approach to study the effects of "pulling" the plug domain out of the barrel.

9. Conclusions

In the past few years, growth in the number of simulation studies and the complexity of the proteins simulated has been phenomenal, and the link between simulation and experiment is becoming stronger in the area of membrane protein simulations. Simulations of pure lipids are now investigating phenomena on much larger length (10–30 nm) and time scales (hundreds of nanoseconds) and can be compared more directly to experiment and theoretical work at mesoscopic scales. Improvements in coarse-grained models show promise for further extensions. Although the availability of fast software and relatively cheap computers will no doubt lead to a further increase in the complexity of the systems that can be simulated, it should also lead to increased methodological development and extensive controls on simulations, as there still is a tendency particularly in complex simulation systems to analyse single observations in great detail. Simulations are generating questions that can be tested experimentally, which will no doubt lead to increasingly stronger links with experiment. The recent growth in the number of high-resolution membrane protein structures is an exciting development. Simulations can provide additional dynamic details of the static snapshots given by membrane protein structures and can be used to investigate and build models of other conformational states. Examples are models and simulations of open and closed states of potassium channels, conformational substates of transporters, and dynamics linking the crystal structures of the different states of bacteriorhodopsin. Further developments in extending the time scale of simulations to slower phenomena and extending the time scale of experiments to faster times to the point they overlap will be very exciting in a wide range of problems involving membrane proteins and lipids.

Acknowledgments

We thank many colleagues for their comments on the manuscript. Although this paper has a long list of references, it is not an exhaustive review and we apologize to our colleagues for omitting some interesting recent papers.

Work in DPT's group is supported by grants from the Canadian Institutes of Health Research and the Natural Sciences and Engineering Research Council.

References

[1] C. Domene, P.J. Bond, M.S. Sansom, Membrane protein simulations: ion channels and bacterial outer membrane proteins, Adv. Protein Chem. 66 (2003) 159–193.
[2] S.E. Feller, Molecular dynamics simulations of lipid bilayers, Curr. Opin. Colloid Interface 5 (2000) 217–223.
[3] L.R. Forrest, M.S.P. Sansom, Membrane simulations: bigger and better? Curr. Opin. Struct. Biol. 10 (2000) 174–181.
[4] R.W. Pastor, Molecular-Dynamics and Monte-Carlo Simulations of Lipid Bilayers, Curr. Opin. Struct. Biol. 4 (1994) 486–492.
[5] H.L. Scott, Modeling the lipid component of membranes, Curr. Opin. Struct. Biol. 12 (2002) 495–502.
[6] D.P. Tieleman, S.J. Marrink, H.J.C. Berendsen, A computer perspective of membranes: molecular dynamics studies of lipid bilayer systems, Biochim. Biophys. Acta 1331 (1997) 235–270.
[7] A.R. Leach, Molecular Modelling: Principles and Applications, 2nd ed., Prentice Hall, Harlow, UK, 2001.
[8] J.W. Ponder, D.A. Case, Force fields for protein simulations, Adv. Protein Chem. 66 (2003) 27–85.
[9] Y.M. Rhee, V.S. Pande, Multiplexed-replica exchange molecular dynamics method for protein folding simulation, Biophys. J. 84 (2003) 775–786.
[10] E. Tajkhorshid, A. Aksimentiev, I. Balabin, M. Gao, B. Isralewitz, J.C. Phillips, F.Q. Zhu, K. Schulten, Large scale simulation of protein mechanics and function, Adv. Protein Chem. 66 (2003) 195–247.
[11] C. Sagui, T.A. Darden, Molecular dynamics simulations of biomolecules: long-range electrostatic effects, Annu. Rev. Biophys. Biomol. 28 (1999) 155–179.
[12] A.F. Voter, Parallel replica method for dynamics of infrequent events, Phys. Rev., B 57 (1998) R13985–R13988.
[13] M. Shirts, V.S. Pande, Computing—screen savers of the world unite!, Science 290 (2000) 1903–1904.
[14] Y. Sugita, Y. Okamoto, Replica-exchange molecular dynamics method for protein folding, Chem. Phys. Lett. 314 (1999) 141–151.
[15] C. Anezo, A.H. de Vries, H.-D. Holtje, D.P. Tieleman, S.J. Marrink, Methodogical issues in lipid bilayer simulations, J. Phys. Chem., B 107 (2003) 9424–9433.
[16] R.A. Bockmann, A. Hac, T. Heimburg, H. Grubmuller, Effect of sodium chloride on a lipid bilayer, Biophys. J. 85 (2003) 1647–1655.
[17] E. Lindahl, O. Edholm, Mesoscopic undulations and thickness fluctuations in lipid bilayers from molecular dynamics simulations, Biophys. J. 79 (2000) 426–433.
[18] S.J. Marrink, A.E. Mark, Effect of undulations on surface tension in simulated bilayers, J. Phys. Chem., B 105 (2001) 6122–6127.
[19] N.V. Eldho, S.E. Feller, S. Tristram-Nagle, I.V. Polozov, K. Gawrisch, Polyunsaturated docosahexaenoic vs. docosapentaenoic acid—differences in lipid matrix properties from the loss of one double bond, J. Am. Chem. Soc. 125 (2003) 6409–6421.
[20] S.E. Feller, K. Gawrisch, A.D. MacKerell Jr., Polyunsaturated fatty acids in lipid bilayers: intrinsic and environmental contributions to

their unique physical properties, J. Am. Chem. Soc. 124 (2002) 318–326.
[21] S.E. Feller, K. Gawrisch, T.B. Woolf, Rhodopsin exhibits a preference for solvation by polyunsaturated docosohexaenoic acid, J. Am. Chem. Soc. 125 (2003) 4434–4435.
[22] T. Huber, K. Rajamoorthi, V.F. Kurze, K. Beyer, M.F. Brown, Structure of docosahexaenoic acid-containing phospholipid bilayers as studied by H-2 NMR and molecular dynamics simulations, J. Am. Chem. Soc. 124 (2002) 298–309.
[23] M.T. Hyvonen, T.T. Rantala, M. AlaKorpela, Structure and dynamic properties of diunsaturated 1-palmitoyl-2-linoleoyl-*sn*-glycero-3-phosphatidylcholine lipid bilayer from molecular dynamics simulation, Biophys. J. 73 (1997) 2907–2923.
[24] L. Saiz, M.L. Klein, Computer simulation studies of model biological membranes, Acc. Chem. Res. 35 (2002) 482–489.
[25] J.J.L. Cascales, J.G. delaTorre, S.J. Marrink, H.J.C. Berendsen, Molecular dynamics simulation of a charged biological membrane, J. Chem. Phys. 104 (1996) 2713–2720.
[26] P. Mukhopadhyay, H.J. Vogel, D.P. Tieleman, Distribution of pentachlorophenol in phospholipid bilayers: a molecular dynamics study, Biophys. J. 86 (2004) 337–345.
[27] S.A. Pandit, M.L. Berkowitz, Molecular dynamics simulation of dipalmitoylphosphatidylserine bilayer with Na^+ counter-ions, Biophys. J. 82 (2002) 1818–1827.
[28] S.W. Chiu, S. Vasudevan, E. Jakobsson, R.J. Mashl, H.L. Scott, Structure of sphingomyelin bilayers: a simulation study, Biophys. J. 85 (2003) 3624–3635.
[29] M.T. Hyvonen, P.T. Kovanen, Molecular dynamics simulation of sphingomyelin bilayer, J. Phys. Chem., B 107 (2003) 9102–9108.
[30] E. Mombelli, R. Morris, W. Taylor, F. Fraternali, Hydrogen-bonding propensities of sphingomyelin in solution and in a bilayer assembly: a molecular dynamics study, Biophys. J. 84 (2003) 1507–1517.
[31] R.D. Lins, T.P. Straatsma, Computer simulation of the rough lipopolysaccharide membrane of *Pseudomonas aeruginosa*, Biophys. J. 81 (2001) 1037–1046.
[32] S. Bandyopadhyay, M. Tarek, M.L. Klein, Molecular dynamics study of a lipid–DNA complex, J. Phys. Chem., B 103 (1999) 10075–10080.
[33] S.J. Marrink, E. Lindahl, O. Edholm, A.E. Mark, Simulation of the spontaneous aggregation of phospholipids into bilayers, J. Am. Chem. Soc. 123 (2001) 8638–8639.
[34] A.H. de Vries, A.E. Mark, S.J. Marrink, Molecular dynamics simulation of the spontaneous formation of a DPPC vesicle in atomistic detail, J. Am. Chem. Soc. 126 (2004) 4488–4489.
[35] D.P. Tieleman, H. Leontiadou, A.E. Mark, S.J. Marrink, Simulation of pore formation in lipid bilayers by mechanical stress and electric fields, J. Am. Chem. Soc. 125 (2003) 6382–6383.
[36] H. Leontiadou, A.E. Mark, S.J. Marrink, Molecular dynamics simulations of hydrophilic pores in lipid bilayers, Biophys. J. 86 (2004) 2156–2164.
[37] D.P. Tieleman, The molecular basis of electroporation, BMC Biochem. 5 (2004) 10.
[38] A. Wierzbicki, P. Dalal, J.D. Madura, H.S. Cheung, Molecular dynamics simulation of crystal-induced membranolysis, J. Phys. Chem., B 107 (2003) 12346–12351.
[39] S.J. Marrink, D.P. Tieleman, Molecular dynamics simulation of a lipid diamond cubic phase, J. Am. Chem. Soc. 123 (2001) 12383–12391.
[40] S.J. Marrink, D.P. Tieleman, Molecular dynamics simulation of spontaneous membrane fusion during a cubic–hexagonal phase transition, Biophys. J. 83 (2002) 2386–2392.
[41] G. Ayton, A.M. Smondyrev, S.G. Bardenhagen, P. McMurtry, G.A. Voth, Interfacing molecular dynamics and macro-scale simulations for lipid bilayer vesicles, Biophys. J. 83 (2002) 1026–1038.
[42] S.J. Marrink, A.E. Mark, Coarse grained model for semi-quantitative lipid simulations, J. Phys. Chem. B 108 (2004) 750–760.
[43] J.C. Shelley, M.Y. Shelley, R.C. Reeder, S. Bandyopadhyay, M.L. Klein, A coarse grain model for phospholipid simulations, J. Phys. Chem., B 105 (2001) 4464–4470.
[44] S.J. Marrink, A.E. Mark, The mechanism of vesicle fusion as revealed by molecular dynamics simulations of small phospholipid vesicles, J. Am. Chem. Soc. 125 (2003) 11144–11145.
[45] M.J. Stevens, J. Hoh, T.B. Woolf, Insights into the molecular mechanism of membrane fusion from simulation: evidence for the association of splayed tails, Phys. Rev. Lett. 91 (2003) 188102.
[46] S.J. Marrink, A.E. Mark, Molecular dynamics simulation of the formation, structure, and dynamics of small phospholipid vesicles, J. Am. Chem. Soc. 125 (2003) 15233–15242.
[47] G. Ayton, G.A. Voth, Bridging microscopic and mesoscopic simulations of lipid bilayers, Biophys. J. 83 (2002) 3357–3370.
[48] A.H. de Vries, A.E. Mark, S.J. Marrink, The binary mixing behavior of phospholipids in a bilayer: a molecular dynamics study, J. Phys. Chem. B 108 (2004) 2454–2463.
[49] S.A. Pandit, D. Bostick, M.L. Berkowitz, Mixed bilayer containing dipalmitoylphosphatidylcholine and dipalmitoylphosphatidylserine: lipid complexation, ion binding, and electrostatics, Biophys. J. 85 (2003) 3120–3131.
[50] S.W. Chiu, E. Jakobsson, R.J. Mashl, H.L. Scott, Cholesterol-induced modifications in lipid bilayers: a simulation study, Biophys. J. 83 (2002) 1842–1853.
[51] C. Hofsass, E. Lindahl, O. Edholm, Molecular dynamics simulations of phospholipid bilayers with cholesterol, Biophys. J. 84 (2003) 2192–2206.
[52] P. Jedlovszky, M. Mezei, Effect of cholesterol on the properties of phospholipid membranes. 1. Structural features, J. Phys. Chem., B 107 (2003) 5311–5321.
[53] T. Rog, M. Pasenkiewicz-Gierula, Effects of epicholesterol on the phosphatidylcholine bilayer: a molecular simulation study, Biophys. J. 84 (2003) 1818–1826.
[54] L. Koubi, M. Tarek, S. Bandyopadhyay, M.L. Klein, D. Scharf, Membrane structural perturbations caused by anesthetics and non-immobilizers: a molecular dynamics investigation, Biophys. J. 81 (2001) 3339–3345.
[55] P. Tang, Y. Xu, Large-scale molecular dynamics simulations of general anesthetic effects on the ion channel in the fully hydrated membrane: the implication of molecular mechanisms of general anesthesia, Proc. Natl. Acad. Sci. U. S. A. 99 (2002) 16035–16040.
[56] A. Grossfield, T.B. Woolf, Interaction of tryptophan analogs with POPC lipid bilayers investigated by molecular dynamics calculations, Langmuir 18 (2002) 198–210.
[57] P. Jedlovszky, M. Mezei, Calculation of the free energy profile of H_2O, O_2, CO, CO_2, NO, and $CHCl_3$ in a lipid bilayer with a cavity insertion variant of the Widom method, J. Am. Chem. Soc. 122 (2000) 5125–5131.
[58] J.L. MacCallum, P. Mukhopadhyay, H. Luo, D.P. Tieleman, Large scale molecular dynamics simulations of lipid-drug interactions, in: D. Senechal (Ed.), Proceedings of the 17th Annual International Symposium on High Performance Computing Systems and Applications and the OSCAR Symposium, NRC Research Press, Ottawa, 2003, pp. 115–122.
[59] S.E. Feller, C.A. Brown, D.T. Nizza, K. Gawrisch, Nuclear Overhauser enhancement spectroscopy cross-relaxation rates and ethanol distribution across membranes, Biophys. J. 82 (2002) 1396–1404.
[60] B. Roux, B. Prodhom, M. Karplus, Ion transport in the gramicidin channel: molecular dynamics study of single and double occupancy, Biophys. J. 68 (1995) 876–892.
[61] Q.F. Zhong, Q. Jiang, P.B. Moore, D.M. Newns, M.L. Klein, Molecular dynamics simulation of a synthetic ion channel, Biophys. J. 74 (1998) 3–10.

[62] A. Grossfield, J. Sachs, T.B. Woolf, Dipole lattice membrane model for protein calculations, Proteins 41 (2000) 211–223.
[63] W. Im, M. Feig, C.L. Brooks, An implicit membrane generalized born theory for the study of structure, stability, and interactions of membrane proteins, Biophys. J. 85 (2003) 2900–2918.
[64] A. Kessel, T. Haliloglu, N. Ben-Tal, Interactions of the M2 delta segment of the acetylcholine receptor with lipid bilayers: a continuum-solvent model study, Biophys. J. 85 (2003) 3687–3695.
[65] T. Lazaridis, Effective energy function for proteins in lipid membranes, Proteins 52 (2003) 176–192.
[66] M.R. de Planque, J.A. Killian, Protein–lipid interactions studied with designed transmembrane peptides: role of hydrophobic matching and interfacial anchoring, Mol. Membr. Biol. 20 (2003) 271–284.
[67] H.I. Petrache, A. Grossfield, K.R. MacKenzie, D.M. Engelman, T.B. Woolf, Modulation of glycophorin A transmembrane helix interactions by lipid bilayers: Molecular dynamics calculations, J. Mol. Biol. 302 (2000) 727–746.
[68] F.I. Valiyaveetil, Y.F. Zhou, R. Mackinnon, Lipids in the structure, folding, and function of the KcsA K^+ channel, Biochemistry 41 (2002) 10771–10777.
[69] J. Baudry, E. Tajkhorshid, F. Molnar, J. Phillips, K. Schulten, Molecular dynamics study of bacteriorhodopsin and the purple membrane, J. Phys. Chem., B 105 (2001) 905–918.
[70] V. Knecht, H. Grubmuller, Mechanical coupling via the membrane fusion SNARE protein syntaxin 1A: a molecular dynamics study, Biophys. J. 84 (2003) 1527–1547.
[71] C. Escrive, M. Laguerre, Molecular dynamics simulations of the insertion of two ideally amphipathic lytic peptides LK15 and LK9 in a 1,2-dimyristoylphosphatidylcholine monolayer, BBA-Biomembranes 1513 (2001) 63–74.
[72] F. Sun, Molecular dynamics simulation of human immunodeficiency virus protein U (Vpu) in lipid/water Langmuir monolayer, J. Mol. Model. 9 (2003) 114–123.
[73] J.A. Freites, Y. Choi, D.J. Tobias, Molecular dynamics simulations of a pulmonary surfactant protein B peptide in a lipid monolayer, Biophys. J. 84 (2003) 2169–2180.
[74] C.E. Nordgren, D.J. Tobias, M.L. Klein, J.K. Blasie, Molecular dynamics simulations of a hydrated protein vectorially oriented on polar and nonpolar soft surfaces, Biophys. J. 83 (2002) 2906–2917.
[75] D.M. Engelman, Y. Chen, C.-N. Chin, A.R. Curran, A.M. Dixon, A.D. Dupuy, A.S. Lee, U. Lehnert, E.E. Matthews, Y.K. Reshetnyak, A. Senes, J.L. Popot, Membrane protein folding: beyond the two stage model, FEBS Lett. 555 (2003) 122–125.
[76] S.H. White, W.C. Wimley, Membrane protein folding and stability: physical principles, Annu. Rev. Biophys. Biomol. 28 (1999) 319–365.
[77] P.D. Adams, D.M. Engelman, A.T. Brunger, Improved prediction for the structure of the dimeric transmembrane domain of glycophorin A obtained through global searching, Proteins 26 (1996) 257–261.
[78] M.S.P. Sansom, H. Weinstein, Hinges, swivels and switches: the role of prolines in signalling via transmembrane alpha-helices, Trends Pharmacol. Sci. 21 (2000) 445–451.
[79] H.S. Son, M.S.P. Sansom, Simulation studies on bacteriorhodopsin alpha-helices, Eur. Biophys. J. Biophys. 28 (2000) 674–682.
[80] P. La Rocca, P.C. Biggin, D.P. Tieleman, M.S.P. Sansom, Simulation studies of the interaction of antimicrobial peptides and lipid bilayers, BBA-Biomembranes 1462 (1999) 185–200.
[81] D.P. Tieleman, M.S.P. Sansom, Molecular dynamics simulations of antimicrobial peptides: from membrane binding to trans-membrane channels, Int. J. Quantum Chem. 83 (2001) 166–179.
[82] W.B. Fischer, M.S.P. Sansom, Viral ion channels: structure and function, BBA-Biomembranes 1561 (2002) 27–45.
[83] M.S.P. Sansom, L.R. Forrest, R. Bull, Viral ion channels: molecular modeling and simulation, BioEssays 20 (1998) 992–1000.
[84] Y. Shai, Mode of action of membrane active antimicrobial peptides, Biopolymers 66 (2002) 236–248.
[85] M. Zasloff, Antimicrobial peptides of multicellular organisms, Nature 415 (2002) 389–395.
[86] P.C. Biggin, M.S.P. Sansom, Interactions of alpha-helices with lipid bilayers: a review of simulation studies, Biophys. Chem. 76 (1999) 161–183.
[87] C.M. Shepherd, H.J. Vogel, D.P. Tieleman, Interactions of the designed antimicrobial peptide MB21 and truncated dermaseptin S3 with lipid bilayers: molecular-dynamics simulations, Biochem. J. 370 (2003) 233–243.
[88] C.M. Shepherd, K.A. Schaus, H.J. Vogel, A.H. Juffer, Molecular dynamics study of peptide-bilayer adsorption, Biophys. J. 80 (2001) 579–596.
[89] L. Monticelli, D. Pedini, E. Schievano, S. Mammi, E. Peggion, Interaction of bombolitin 11 with a membrane-mimetic environment: an NMR and molecular dynamics simulation approach, Biophys. Chem. 101 (2002) 577–591.
[90] W.N. Huang, S.C. Sue, D.S. Wang, P.L. Wu, W.G. Wu, Peripheral binding mode and penetration depth of cobra cardiotoxin on phospholipid membranes as studied by a combined FTIR and computer simulation approach, Biochemistry 42 (2003) 7457–7466.
[91] S. Kamath, T.C. Wong, Membrane structure of the human immunodeficiency virus gp41 fusion domain by molecular dynamics simulation, Biophys. J. 83 (2002) 135–143.
[92] T.C. Wong, Membrane structure of the human immunodeficiency virus gp41 fusion peptide by molecular dynamics simulation II. The glycine mutants, BBA-Biomembranes 1609 (2003) 45–54.
[93] M.P. Aliste, J.L. MacCallum, D.P. Tieleman, Molecular dynamics simulations of pentapeptides at interfaces: salt bridge and cation–pi interactions, Biochemistry 42 (2003) 8976–8987.
[94] E.A. Dolan, R.M. Venable, R.W. Pastor, B.R. Brooks, Simulations of membranes and other interfacial systems using *P*2 (1) and pc periodic boundary conditions, Biophys. J. 82 (2002) 2317–2325.
[95] W.C. Wimley, K. Gawrisch, T.P. Creamer, S.H. White, Direct measurement of salt-bridge solvation energies using a peptide model system: Implications for protein stability, Proc. Natl. Acad. Sci. U. S. A. 93 (1996) 2985–2990.
[96] R. Sankararamakrishnan, H. Weinstein, Positioning and stabilization of dynorphin peptides in membrane bilayers: the mechanistic role of aromatic and basic residues revealed from comparative MD simulations, J. Phys. Chem., B 106 (2002) 209–218.
[97] R. Sankararamakrishnan, H. Weinstein, Molecular dynamics simulations predict a tilted orientation for the helical region of dynorphin A(1–17) in dimyristoylphosphatidylcholine bilayers, Biophys. J. 79 (2000) 2331–2344.
[98] C. Chipot, B. Maigret, A. Pohorille, Early events in the folding of an amphipathic peptide: a multinanosecond molecular dynamics study, Proteins 36 (1999) 383–399.
[99] C. Chipot, A. Pohorille, Folding and translocation of the undecamer of poly-L-leucine across the water–hexane interface. A molecular dynamics study, J. Am. Chem. Soc. 120 (1998) 11912–11924.
[100] R. Zangi, M.L. de Vocht, G.T. Robillard, A.E. Mark, Molecular dynamics study of the folding of hydrophobin SC3 at a hydrophilic/hydrophobic interface, Biophys. J. 83 (2002) 112–124.
[101] V. Khutorsky, alpha-hairpin stability and folding of transmembrane segments, Biochem. Biophys. Res. Commun. 301 (2003) 31–34.
[102] M. Prevost, I. Ortmans, Interactions of the N-terminal domain of apolipoprotein E with a mimetic water–lipid surface: a molecular dynamics study, J. Phys. Chem., B 105 (2001) 7080–7086.
[103] A.M. Dixon, R.M. Venable, R.W. Pastor, T.E. Bull, Micelle-bound conformation of a hairpin-forming peptide: combined NMR and molecular dynamics study, Biopolymers 65 (2002) 284–298.
[104] X.F. Gao, T.C. Wong, Molecular dynamics simulation of adrenocorticotropin (1–10) peptide in a solvated dodecylphosphocholine micelle, Biopolymers 58 (2001) 643–659.
[105] M. Nina, S. Berneche, B. Roux, Anchoring of a monotopic membrane protein: the binding of prostaglandin H-2 synthase-1 to

the surface of a phospholipid bilayer, Eur. Biophys. J. Biophys. 29 (2000) 439–454.
[106] K. Gupta, B.S. Selinsky, C.J. Kaub, A.K. Katz, P.J. Loll, The 2.0 A resolution crystal structure of prostaglandin H-2 synthase-1: structural insights into an unusual peroxidase, J. Mol. Biol. 335 (2004) 503–518.
[107] S.M. Singh, D. Murray, Molecular modeling of the membrane targeting of phospholipase C pleckstrin homology domains, Protein Sci. 12 (2003) 1934–1953.
[108] K. Diraviyam, R.V. Stahelin, W. Cho, D. Murray, Computer modeling of the membrane interaction of FYVE domains, J. Mol. Biol. 328 (2003) 721–736.
[109] J.N. Bright, M.S.P. Sansom, The flexing/twirling helix: exploring the flexibility about molecular hinges formed by proline and glycine motifs in transmembrane helices, J. Phys. Chem., B 107 (2003) 627–636.
[110] T.H. Duong, E.L. Mehler, H. Weinstein, Molecular dynamics simulation of membranes and a transmembrane helix, J. Comput. Phys. 151 (1999) 358–387.
[111] M. Olivella, X. Deupi, C. Govaerts, L. Pardo, Influence of the environment in the conformation of alpha-helices studied by protein database search and molecular dynamics simulations, Biophys. J. 82 (2002) 3207–3213.
[112] H.I. Petrache, D.M. Zuckerman, J.N. Sachs, J.A. Killian, R.E. Koeppe, T.B. Woolf, Hydrophobic matching mechanism investigated by molecular dynamics simulations, Langmuir 18 (2002) 1340–1351.
[113] T. Stockner, W.L. Ash, J.L. MacCallum, D.P. Tieleman, Direct simulation of transmembrane helix association: role of asparagines, Biophys. J. (2004) (in press).
[114] L.R. Forrest, T.B. Woolf, Discrimination of native loop conformations in membrane proteins: decoy library design and evaluation of effective energy scoring functions, Proteins 52 (2003) 492–509.
[115] L.R. Forrest, D.P. Tieleman, M.S.P. Sansom, Defining the transmembrane helix of M2 protein from influenza A by molecular dynamics simulations in a lipid bilayer, Biophys. J. 76 (1999) 1886–1896.
[116] J.N. Bright, I.H. Shrivastava, F.S. Cordes, M.S.P. Sansom, Conformational dynamics of helix S6 from Shaker potassium channel: simulation studies, Biopolymers 64 (2002) 303–313.
[117] I.H. Shrivastava, C.E. Capener, L.R. Forrest, M.S.P. Sansom, Structure and dynamics of K channel pore-lining helices: a comparative simulation study, Biophys. J. 78 (2000) 79–92.
[118] D.P. Tieleman, I.H. Shrivastava, M.R. Ulmschneider, M.S.P. Sansom, Proline-induced hinges in transmembrane helices: possible roles in ion channel gating, Proteins 44 (2001) 63–72.
[119] O. Beckstein, P.C. Biggin, P. Bond, J.N. Bright, C. Domene, A. Grottesi, J. Holyoake, M.S.P. Sansom, Ion channel gating: insights via molecular simulations, FEBS Lett. 555 (2003) 85–90.
[120] F.S. Cordes, J.N. Bright, M.S.P. Sansom, Proline-induced distortions of transmembrane helices, J. Mol. Biol. 323 (2002) 951–960.
[121] C. Govaerts, C. Blanpain, X. Deupi, S. Ballet, J.A. Ballesteros, S.J. Wodak, G. Vassart, L. Pardo, M. Parmentier, The TXP motif in the second transmembrane helix of CCR5—structural determinant of chemokine-induced activation, J. Biol. Chem. 276 (2001) 13217–13225.
[122] X. Deupi, M. Olivella, C. Govaerts, J.A. Ballesteros, M. Campillo, L. Pardo, Ser and Thr residues modulate the conformation of pro-kinked transmembrane alpha-helices, Biophys. J. 86 (2004) 105–115.
[123] R.J. Law, L.R. Forrest, K.M. Ranatunga, P. La Rocca, D.P. Tieleman, M.S.P. Sansom, Structure and dynamics of the pore-lining helix of the nicotinic receptor: MD simulations in water, lipid bilayers, and transbilayer bundles, Proteins 39 (2000) 47–55.
[124] R.J. Law, D.P. Tieleman, M.S.P. Sansom, Pores formed by the nicotinic receptor M2 delta peptide: a molecular dynamics simulation study, Biophys. J. 84 (2003) 14–27.
[125] A. Kessel, D. Shental-Bechor, T. Haliloglu, N. Ben-Tal, Interactions of hydrophobic peptides with lipid bilayers: Monte Carlo simulations with M2 delta, Biophys. J. 85 (2003) 3431–3444.
[126] R. Jahn, H. Grubmuller, Membrane fusion, Curr. Opin. Cell Biol. 14 (2002) 488–495.
[127] D. Fasshauer, Structural insights into the SNARE mechanism, BBA-Mol. Cell Res. 1641 (2003) 87–97.
[128] X. Han, C.-T. Wang, J. Bai, E.R. Chapman, M.B. Jackson, Transmembrane segments of syntaxin line the fusion pore of Ca^{2+}-triggered exocytosis, Science (2004) 1095801.
[129] W.F. DeGrado, H. Gratkowski, J.D. Lear, How do helix–helix interactions help determine the folds of membrane proteins? Perspectives from the study of homo-oligomeric helical bundles, Protein Sci. 12 (2003) 647–665.
[130] K.E. Gottschalk, P.D. Adams, A.T. Brunger, H. Kessler, Transmembrane signal transduction of the alpha(IIb)beta(3) integrin, Protein Sci. 11 (2002) 1800–1812.
[131] U. Kochva, H. Leonov, I.T. Arkin, Modeling the structure of the respiratory syncytial virus small hydrophobic protein by silent-mutation analysis of global searching molecular dynamics, Protein Sci. 12 (2003) 2668–2674.
[132] J. Torres, J.A.G. Briggs, I.T. Arkin, Contribution of energy values to the analysis of global searching molecular dynamics simulations of transmembrane helical bundles, Biophys. J. 82 (2002) 3063–3071.
[133] J. Torres, J.A.G. Briggs, I.T. Arkin, Convergence of experimental, computational and evolutionary approaches predicts the presence of a tetrameric form for CD3-zeta, J. Mol. Biol. 316 (2002) 375–384.
[134] S. Kim, A.K. Chamberlain, J.U. Bowie, A simple method for modeling transmembrane helix oligomers, J. Mol. Biol. 329 (2003) 831–840.
[135] C.T. Choma, D.P. Tieleman, D. Cregut, L. Serrano, H.J.C. Berendsen, Towards the design and computational characterization of a membrane protein, J. Mol. Graph. Model. 20 (2001) 219–234.
[136] S.J. Fleishman, N. Ben-Tal, A novel scoring function for predicting the conformations of tightly packed pairs of transmembrane alpha-helices, J. Mol. Biol. 321 (2002) 363–378.
[137] S.J. Fleishman, J. Schlessinger, N. Ben-Tal, A putative molecular-activation switch in the transmembrane domain of erbB2, Proc. Natl. Acad. Sci. U. S. A. 99 (2002) 15937–15940.
[138] N. BenTal, B. Honig, Helix–helix interactions in lipid bilayers, Biophys. J. 71 (1996) 3046–3050.
[139] K. Bohinc, V. Kralj-Iglic, S. May, Interaction between two cylindrical inclusions in a symmetric lipid bilayer, J. Chem. Phys. 119 (2003) 7435–7444.
[140] A. Zemel, D.R. Fattal, A. Ben-Shaul, Energetics and self-assembly of amphipathic peptide pores in lipid membranes, Biophys. J. 84 (2003) 2242–2255.
[141] M.E. Gonzalez, L. Carrasco, Viroporins, FEBS Lett. 552 (2003) 28–34.
[142] A. Pohorille, M.A. Wilson, C. Chipot, Membrane peptides and their role in protobiological evolution, Orig. Life Evol. Biosph. 33 (2003) 173–197.
[143] W.B. Fischer, Vpu from HIV-1 on an atomic scale: experiments and computer simulations, FEBS Lett. 552 (2003) 39–46.
[144] C.H. Yu, S. Cukierman, R. Pomes, Theoretical study of the structure and dynamic fluctuations of dioxolane-linked gramicidin channels, Biophys. J. 84 (2003) 816–831.
[145] J.D. Lear, Proton conduction through the M2 protein of the influenza A virus; a quantitative, mechanistic analysis of experimental data, FEBS Lett. 552 (2003) 17–22.
[146] J.D. Lear, Z.R. Wasserman, W.F. DeGrado, Synthetic amphiphilic peptide models for protein ion channels., Science 240 (1988) 1177–1181.
[147] R. Pomes, B. Roux, Molecular mechanism of H^+ conduction in the single-file water chain of the gramicidin channel, Biophys. J. 82 (2002) 2304–2316.

[148] C.H. Yu, R. Pomes, Functional dynamics of ion channels: modulation of proton movement by conformational switches, J. Am. Chem. Soc. 125 (2003) 13890–13894.
[149] F.H. Stillinger, C.W. David, Polarization model for water and its ionic dissociation products, J. Chem. Phys. 69 (1978) 1473–1484.
[150] Y.J. Wu, G.A. Voth, A computer simulation study of the hydrated proton in a synthetic proton channel, Biophys. J. 85 (2003) 864–875.
[151] A.M. Smondyrev, G.A. Voth, Molecular dynamics simulation of proton transport through the influenza A virus M2 channel, Biophys. J. 83 (2002) 1987–1996.
[152] A. Warshel, Molecular dynamics simulations of biological reactions, Acc. Chem. Res. 35 (2002) 385–395.
[153] H.S. Randa, L.R. Forrest, G.A. Voth, M.S.P. Sansom, Molecular dynamics of synthetic leucine–serine ion channels in a phospholipid membrane, Biophys. J. 77 (1999) 2400–2410.
[154] Q. Zhong, Q. Jiang, P.B. Moore, D.M. Newns, M.L. Klein, Molecular dynamics simulation of an ion channel, Biophys. J. 74 (1998) 3–10.
[155] G.A. Woolley, B.A. Wallace, Model ion channels: gramicidin and alamethicin, J. Membr. Biol. 129 (1992) 109–136.
[156] D.P. Tieleman, H.J.C. Berendsen, M.S.P. Sansom, Voltage-dependent insertion of alamethicin at phospholipid/water and octane/water interfaces, Biophys. J. 80 (2001) 331–346.
[157] B. Bechinger, Structure and function of channel-forming peptides: magainins, cecrpins, melittin and alamethicin, J. Membr. Biol. 156 (1997) 197–211.
[158] D.P. Tieleman, P.C. Biggin, G.R. Smith, M.S. Sansom, Simulation approaches to ion channel structure–function relationships, Q. Rev. Biophys. 34 (2001) 473–561.
[159] D. Bostick, M.L. Berkowitz, The implementation of slab geometry for membrane-channel molecular dynamics simulations, Biophys. J. 85 (2003) 97–107.
[160] D.P. Tieleman, B. Hess, M.S.P. Sansom, Analysis and evaluation of channel models: Simulations of alamethicin, Biophys. J. 83 (2002) 2393–2407.
[161] D.P. Tieleman, in: S. Bezrukov (Ed.), Unsolved problems in noise and fluctuations III, AIP Proceedings 665, Molecular motions in ion channels: a possible link to noise in single channels, American Institute of Physics, New York, 2003, pp. 298–304.
[162] A. Kessel, D.P. Tieleman, N. Ben-Tal, Implicit solvent model estimates of the stability of model structures of the alamethicin channel, Eur. Biophys. J. 33 (2004) 16–28.
[163] A.V. Starostin, R. Butan, V. Borisenko, D.A. James, H. Wenschuh, M.S. Sansom, G.A. Woolley, An anion-selective analogue of the channel-forming peptide alamethicin, Biochemistry 38 (1999) 6144–6150.
[164] D.P. Tieleman, V. Borisenko, M.S. Sansom, G.A. Woolley, Understanding pH-dependent selectivity of alamethicin K18 channels by computer simulation, Biophys. J. 84 (2003) 1464–1469.
[165] T. Okada, K. Palczewski, Crystal structure of rhodopsin: implications for vision and beyond, Curr. Opin. Struct. Biol. 11 (2001) 420–426.
[166] M. Garavelli, F. Bernardi, M.A. Roob, M. Olivucci, Computer simulation of photoinduced molecular motion and reactivity, Int. J. Photoenergy 4 (2002) 57–68.
[167] A.D. Albert, P.L. Yeagle, Structural studies on rhodopsin, Biochim. Biophys. Acta 1565 (2002) 183–195.
[168] K. Palczewski, T. Kumasaka, T. Hori, C.A. Behnke, H. Motoshima, B.A. Fox, I.L. Trong, D.C. Teller, T. Okada, R.E. Stenkamp, M. Yamamoto, M. Miyano, Crystal structure of rhodopsin: a G-protein-coupled receptor, Science 289 (2000) 739–745.
[169] C. Bissantz, P. Bernard, M. Hibert, D. Rognan, Protein-based virtual screening of chemiscal databases: II. Are homology models of G-protein coupled receptors suitable targets? Proteins 50 (2003) 5–25.
[170] J.J. Chambers, D.E. Nichols, A homology-based model of the human 5-HT_{2A} receptor derived from an in silico activated G-protein coupled receptor, J. Comput.-Aided Mol. Des. 16 (2002) 511–520.
[171] S. Filipek, R.E. Stenkamp, D.C. Teller, K. Palczewski, G-Protein-coupled receptor phodopsin: a prospectus, Annu. Rev. Physiol. 65 (2003) 851–879.
[172] S. Filipek, D.C. Teller, K. Palczewski, R. Stenkamp, The crystallographic model of rhodopsin and its use in studies of other G-protein coupled receptors, Annu. Rev. Biophys. Biomol. 32 (2003) 375–397.
[173] A. Gieldon, R. Kazmierkiewicz, R. Slusarz, M. Pasenkiewicz-Gierula, J. Ciarkowski, Molecular dynamics study of 4-OH-phenylacetyl-D-Y(Me)FQNRPR-NH_2 selectivity to V1a receptor, J. Mol. Model. 9 (2003) 372–378.
[174] X. Huang, J. Shen, M. Cui, L. Shen, X. Luo, K. Ling, G. Pei, H. Jiang, K. Chen, Molecular dynamics simulations on SDF-1α: binding with CSCR4 receptor, Biophys. J. 84 (2003) 171–184.
[175] S.-K. Kim, Z.-G. Gao, P. Van Rompaey, A.S. Gross, A. Chen, S. Van Calenbergh, K.A. Jacobson, Modeling the adenosine receptors: comparison of the binding domains of A_{2A} agonists and antagonists, J. Med. Chem. 46 (2003) 4847–4859.
[176] J. Klein-Seetharaman, Dynamics in rhodopsin, ChemBioChem 3 (2002) 981–986.
[177] S. Moro, F. Deflorian, G. Spalluto, G. Pastorin, B. Cacciari, S.-K. Kim, K.A. Jacobson, Demystifying the three dimensional structure of G protein-coupled receptors (GPCRs) with the aid of molecular modeling, Chem. Commun. (2003) 2949–2956.
[178] J.O. Trent, Z.-X. Wang, J.L. Murray, W. Shao, H. Tamamura, N. Fujii, S.C. Peiper, Lipid bilayer simulations of CXCR4 with inverse agonists and weak partial agonists, J. Biol. Chem. 278 (2003) 47136–47144.
[179] X.-Q. Xie, J.-Z. Chen, E.M. Billings, 3D structural model of the G-protein-coupled cannabinoid CB_2 receptor, Proteins 53 (2003) 307–319.
[180] X. Yang, Z. Want, W. Dong, L. Ling, H. Yang, R. Chen, Modeling and docking of the three-dimensional structure of the human melanocortin 4 receptor, J. Protein Chem. 22 (2003) 334–344.
[181] P.S. Crozier, M.J. Stevens, L.R. Forrest, T.B. Woolf, Molecular dynamics simulations of dark-adapted rhodopsin in an explicit membrane bilayer: coupling between local retinal and larger scale conformational change, J. Mol. Biol. 333 (2003) 493–514.
[182] U. Rohrig, L. Guidoni, U. Rothlisberger, Early steps of the intramolecular signal transduction in rhodopsin explored by molecular dynamics simulations, Biochemistry 41 (2002) 10799–10809.
[183] J. Saam, E. Tajkhorshid, S. Hayashi, K. Schulten, Molecular dynamics investigation of primary photoinduced events in the activation of rhodopsin, Biophys. J. 83 (2002) 3097–3112.
[184] G. Choi, J. Landin, J.F. Galan, R.R. Birge, A.D. Albert, P.L. Yeagle, Structural studies of metarhodopsin II, the activated form of the G-protein coupled receptor, Rhodopsin, Biochemistry 41 (2002) 7318–7324.
[185] R. Henderson, J.M. Baldwin, T.A. Ceska, F. Zemlin, E. Beckmann, K.H. Downing, Model for the Structure of bacteriorhodopsin based on high-resolution electron cryo-microscopy, J. Mol. Biol. 213 (1990) 899–929.
[186] M. Nonella, A. Windemuth, K. Schulten, Structure of bacteriorhodopsin and in situ isomerization of retinal: a molecular dynamics study, Photochem. Photobiol. 54 (1991) 937–948.
[187] O. Edholm, O. Berger, F. Jahnig, Structure and fluctuations of bacteriorhodopsin in the purple membrane: a molecular dynamics study, J. Mol. Biol. 250 (1995) 95–111.
[188] S. Hayashi, E. Tajkhorshid, K. Schulten, Molecular dynamics simulation of bacteriorhodopsin's photoisomerization using ab initio forces for the excited chromophore, Biophys. J. 85 (2003) 1440–1449.
[189] K. Murata, K. Mitsuoaka, T. Hirai, T. Walz, P. Agre, J.B. Heymann, A. Engel, Y. Fujiyoshi, Structural determinants of water permeation through aquaporin-1, Nature 407 (2000) 599–605.
[190] G. Ren, V.S. Reddy, A. Cheng, P. Melnyk, A.K. Mitra, Visualization of a water-selective pore by electron crystallography in vitreous ice, Proc. Natl. Acad. Sci. U. S. A. 98 (2001) 1398–1403.

[191] D. Fu, A. Libson, L.J.W. Miercke, C. Weitzman, P. Nollert, J. Krucinski, R.M. Stroud, Structure of a glycerol-conducting channel and the basis for its selectivity, Science 290 (2000) 481–486.
[192] B.L. de Groot, A. Engel, H. Grubmuller, The structure of the aquaporin-1 water channel: a comparison between cryo-electron microscopy and X-ray crystallography, J. Mol. Biol. 325 (2003) 485–493.
[193] Y. Fujiyoshi, K. Mitsuoka, B.L. de Groot, A. Philippsen, H. Grubmuller, P. Agre, A. Engel, Structure and function of water channels, Curr. Opin. Struct. Biol. 12 (2002) 509–515.
[194] R.J. Law, M.S.P. Sansom, Water transporters: how so fast yet so selective? Curr. Biol. 12 (2002) R250–R252.
[195] R.M. Stroud, L.J.W. Miercke, J. O'Connell, S. Khademi, J.K. Lee, J. Remis, W. Harries, Y. Robles, D. Akhavan, Glycerol facilitator GlpF and the associated aquaporin family of channels, Curr. Opin. Struct. Biol. 13 (2003) 424–431.
[196] B.L. de Groot, T. Frigato, V. Helms, H. Grubmuller, The mechanism of proton exclusion in the aquaporin-1 water channel, J. Mol. Biol. 333 (2003) 279–293.
[197] B.L. de Groot, A. Engel, H. Grubmuller, A refined structure of human aquaporin-1, FEBS Lett. 504 (2001) 206–211.
[198] F.Q. Zhu, E. Tajkhorshid, K. Schulten, Molecular dynamics study of aquaporin-1 water channel in a lipid bilayer, FEBS Lett. 504 (2001) 212–218.
[199] B.L. de Groot, H. Grubmuller, Water permeation across biological membranes: Mechanism and dynamics of aquaporin-1 and GlpF, Science 294 (2001) 2353–2357.
[200] E. Tajkhorshid, P. Nollert, M.O. Jensen, L.J.W. Miercke, J. O'Connell, R.M. Stroud, K. Schulten, Control of the selectivity of the aquaporin water channel family by global orientational tuning, Science 296 (2002) 525–530.
[201] M.O. Jensen, E. Tajkhorshid, K. Schulten, Electrostatic tuning of permeation and selectivity in aquaporin water channels, Biophys. J. 85 (2003) 2884–2899.
[202] F.Q. Zhu, E. Tajkhorshid, K. Schulten, Pressure-induced water transport in membrane channels studied by molecular dynamics, Biophys. J. 83 (2002) 154–160.
[203] F.Q. Zhu, E. Tajkhorshid, K. Schulten, Theory and simulation of water permeation in Aquaporin-1, Biophys. J. 86 (2004) 50–57.
[204] M.O. Jensen, E. Tajkhorshid, K. Schulten, The mechanism of glycerol conduction in aquaglyceroporins, Structure 9 (2001) 1083–1093.
[205] M.O. Jensen, S. Park, E. Tajkhorshid, K. Schulten, Energetics of glycerol conduction through aquaglyceroporin GlpF, Proc. Natl. Acad. Sci. U. S. A. 99 (2002) 6731–6736.
[206] D.Y. Lu, P. Grayson, K. Schulten, Glycerol conductance and physical asymmetry of the *Escherichia coli* glycerol facilitator GlpF, Biophys. J. 85 (2003) 2977–2987.
[207] P. Grayson, E. Tajkhorshid, K. Schulten, Mechanisms of selectivity in channels and enzymes studied with interactive molecular dynamics, Biophys. J. 85 (2003) 36–48.
[208] A. Burykin, A. Warshel, What really prevents proton transport through aquaporin? Charge self-energy versus proton wire proposals, Biophys. J. 85 (2003) 3696–3706.
[209] M.A. Lill, V. Helms, Molecular dynamics simulation of proton transport with quantum mechanically derived proton hopping rates (Q-HOP MD), J. Chem. Phys. 115 (2001) 7993–8005.
[210] F. Zhu, K. Schulten, Water and proton conduction through carbon nanotubes as models for biological channels, Biophys. J. 85 (2003) 236–244.
[211] N. Chakrabarti, E. Tajkhorshid, B. Roux, R. Pomes, Molecular basis of proton blockage in aquaporins, Structure 12 (2004) 65–74.
[212] T.J.F. Day, A.V. Soudackov, M. Cuma, U.W. Schmitt, G.A. Voth, A second generation multistate empirical valence bond model for proton transport in aqueous systems, J. Chem. Phys. 117 (2002) 5839–5849.
[213] B. Ilan, E. Tajkhorshid, K. Schulten, G.A. Voth, The mechanism of proton exclusion in aquaporin channels, Proteins 55 (2004) 223–228.
[214] D.A. Doyle, J.M. Cabral, R.A. Pfuetzner, A.L. Kuo, J.M. Gulbis, S.L. Cohen, B.T. Chait, R. MacKinnon, The structure of the potassium channel: molecular basis of K^+ conduction and selectivity, Science 280 (1998) 69–77.
[215] C. Domene, M.S. Sansom, Potassium channel, ions, and water: simulation studies based on the high resolution X-ray structure of KcsA, Biophys. J. 85 (2003) 2787–2800.
[216] Y. Zhou, J.H. Morais-Cabral, A. Kaufman, R. MacKinnon, Chemistry of ion coordination and hydration revealed by a K^+ channel-Fab complex at 2.0 A resolution, Nature 414 (2001) 43–48.
[217] Y. Jiang, A. Lee, J. Chen, M. Cadene, B.T. Chait, R. MacKinnon, The open pore conformation of potassium channels, Nature 417 (2002) 523–526.
[218] J. Cohen, K. Schulten, Mechanism of anionic conduction across ClC, Biophys. J. 86 (2004) 836–845.
[219] B. Corry, M. O'Mara, S.H. Chung, Conduction mechanisms of chloride ions in ClC-type channels, Biophys. J. 86 (2004) 846–860.
[220] R. Dutzler, E.B. Campbell, M. Cadene, B.T. Chait, R. MacKinnon, X-ray structure of a CIC chloride channel at 3.0 angstrom reveals the molecular basis of anion selectivity, Nature 415 (2002) 287–294.
[221] G.V. Miloshevsky, P.C. Jordan, Anion pathway and potential energy profiles along curvilinear bacterial ClC Cl(−) pores: electrostatic effects of charged residues, Biophys. J. 86 (2004) 825–835.
[222] Y. Jiang, A. Lee, J. Chen, V. Ruta, M. Cadene, B.T. Chait, R. MacKinnon, X-ray structure of a voltage-dependent K^+ channel, Nature 423 (2003) 33–41.
[223] Y. Jiang, V. Ruta, J. Chen, A. Lee, R. MacKinnon, The principle of gating charge movement in a voltage-dependent K^+ channel, Nature 423 (2003) 42–48.
[224] L. Monticelli, K.M. Robertson, J.L. MacCallum, D.P. Tieleman, Computer simulation of the KvAP voltage-gated potassium channel: steered molecular dynamics of the voltage sensor, FEBS Lett. 564 (2004) 325–332.
[225] A. Kuo, J.M. Gulbis, J.F. Antcliff, T. Rahman, E.D. Lowe, J. Zimmer, J. Cuthbertson, F.M. Ashcroft, T. Ezaki, D.A. Doyle, Crystal structure of the potassium channel KirBac1.1 in the closed state, Science 300 (2003) 1922–1926.
[226] M.S.P. Sansom, I.H. Shrivastava, J.N. Bright, J. Tate, C.E. Capener, P.C. Biggin, Potassium channels: structures, models, simulations, BBA-Biomembranes 1565 (2002) 294–307.
[227] M.S.P. Sansom, I.H. Shrivastava, K.M. Ranatunga, G.R. Smith, Simulations of ion channels—watching ions and water move, Trends Biochem. Sci. 25 (2000) 368–374.
[228] B. Roux, S. Berneche, W. Im, Ion channels, permeation, and electrostatics: insight into the function of KcsA, Biochemistry 39 (2000) 13295–13306.
[229] B. Roux, Theoretical and computational models of ion channels, Curr. Opin. Struct. Biol. 12 (2002) 182–189.
[230] B. Hille, Ionic Channels of Excitable Membranes, 3rd ed., Sinauer Associates, Sunderland, Mass, 2002.
[231] S. Kuyucak, O.S. Andersen, S.-H. Chung, Models of permeation in ion channels, Rep. Prog. Phys. 64 (2001) 1427–1472.
[232] B. Roux, Computational studies of the gramicidin channel, Acc. Chem. Res. 35 (2002) 366–375.
[233] B.L. de Groot, D.P. Tieleman, P. Pohl, H. Grubmuller, Water permeation through gramicidin A: desformylation and the double helix; a molecular dynamics study, Biophys. J. 82 (2002) 2934–2942.
[234] G.V. Miloshevsky, P.C. Jordan, Gating gramicidin channels in lipid bilayers: reaction coordinates and the mechanism of dissociation, Biophys. J. 86 (2004) 92–104.
[235] R. Ketchem, B. Roux, T. Cross, High-resolution polypeptide structure in a lamellar phase lipid environment from solid state NMR derived orientational constraints, Structure 5 (1997) 1655–1669.
[236] L.E. Townsley, W.A. Tucker, S. Sham, J.F. Hinton, Structures of gramicidins A, B, and C incorporated into sodium dodecyl sulfate micelles, Biochemistry 40 (2001) 11676–11686.

[237] T.W. Allen, O.S. Andersen, B. Roux, Structure of gramicidin A in a lipid bilayer environment determined using molecular dynamics simulations and solid-state NMR data, J. Am. Chem. Soc. 125 (2003) 9868–9877.
[238] T.W. Allen, T. Bastug, S. Kuyucak, S.H. Chung, Gramicidin A channel as a test ground for molecular dynamics force fields, Biophys. J. 84 (2003) 2159–2168.
[239] T.W. Allen, O.S. Andersen, B. Roux, Energetics of ion conduction through the gramicidin channel, Proc. Natl. Acad. Sci. U. S. A. 101 (2004) 117–122.
[240] S. Edwards, B. Corry, S. Kuyucak, S.H. Chung, Continuum electrostatics fails to describe ion permeation in the gramicidin channel, Biophys. J. 83 (2002) 1348–1360.
[241] B. Corry, S. Kuyucak, S.H. Chung, Dielectric self-energy in Poisson–Boltzmann and Poisson–Nernst–Planck models of ion channels, Biophys. J. 84 (2003) 3594–3606.
[242] A.B. Mamonov, R.D. Coalson, A. Nitzan, M.G. Kurnikova, The role of the dielectric barrier in narrow biological channels: A novel composite approach to modeling single-channel currents, Biophys. J. 84 (2003) 3646–3661.
[243] M. Tarek, B. Maigret, C. Chipot, Molecular dynamics investigation of an oriented cyclic peptide nanotube in DMPC bilayers, Biophys. J. 85 (2003) 2287–2298.
[244] E. Perozo, D.C. Rees, Structure and mechanism in prokaryotic mechanosensitive channels, Curr. Opin. Struct. Biol. 13 (2003) 432–442.
[245] R.B. Bass, K.P. Locher, E. Borths, Y. Poon, P. Strop, A. Lee, D.C. Rees, The structures of BtuCD and MscS and their implications for transporter and channel function, FEBS Lett. 555 (2003) 111–115.
[246] F. Bezanilla, E. Perozo, The voltage sensor and the gate in ion channels, Adv. Protein Chem. 63 (2003) 211–241.
[247] A. Anishkin, V. Gendel, N.A. Sharifi, C.S. Chiang, L. Shirinian, H.R. Guy, S. Sukharev, On the conformation of the COOH-terminal Domain of the Large Mechanosensitive Channel MscL, J. Gen. Physiol. 121 (2003) 227–244.
[248] D.E. Elmore, D.A. Dougherty, Molecular dynamics simulations of wild-type and mutant forms of the *Mycobacterium tuberculosis* MscL channel, Biophys. J. 81 (2001) 1345–1359.
[249] J. Gullingsrud, D. Kosztin, K. Schulten, Structural determinants of MscL gating studied by molecular dynamics simulations, Biophys. J. 80 (2001) 2074–2081.
[250] L.E. Bilston, K. Mylvaganam, Molecular simulations of the large conductance mechanosensitive (MscL) channel under mechanical loading, FEBS Lett. 512 (2002) 185–190.
[251] G. Colombo, S.J. Marrink, A.E. Mark, Simulation of MscL Gating in a bilayer under stress, Biophys. J. 84 (2003) 2331–2337.
[252] J. Gullingsrud, K. Schulten, Gating of MscL studied by steered molecular dynamics, Biophys. J. 85 (2003) 2087–2099.
[253] M. Betanzos, C.S. Chiang, H.R. Guy, S. Sukharev, A large iris-like expansion of a mechanosensitive channel protein induced by membrane tension, Nat. Struct. Biol. 9 (2002) 704–710.
[254] S. Sukharev, S.R. Durell, H.R. Guy, Structural Models of the MscL Gating Mechanism, Biophys. J. 81 (2001) 917–936.
[255] E. Perozo, D.M. Cortes, P. Sompornpisut, A. Kloda, B. Martinac, Open channel structure of MscL and the gating mechanism of mechanosensitive channels, Nature 418 (2002) 942–948.
[256] H. Valadie, J.J. Lacapcre, Y.H. Sanejouand, C. Etchebest, Dynamical properties of the MscL of *Escherichia coli*: a normal mode analysis, J. Mol. Biol. 332 (2003) 657–674.
[257] I.H. Shrivastava, D.P. Tieleman, P.C. Biggin, M.S.P. Sansom, K^+ versus Na^+ ions in a K channel selectivity filter: A simulation study, Biophys. J. 83 (2002) 633–645.
[258] Y. Zhou, R. MacKinnon, The occupancy of ions in the K^+ selectivity filter: charge balance and coupling of ion binding to a protein conformational change underlie high conduction rates, J. Mol. Biol. 333 (2003) 965–975.
[259] B. Roux, S. Berneche, On the potential functions used in molecular dynamics simulations of ion channels, Biophys. J. 82 (2002) 1681–1684.
[260] A. Grossfield, P. Ren, J.W. Ponder, Ion solvation thermodynamics from simulation with a polarizable force field, J. Am. Chem. Soc. 125 (2003) 15671–15682.
[261] S. Berneche, B. Roux, Energetics of ion conduction through the K^+ channel, Nature 414 (2001) 73–77.
[262] A. Burykin, M. Kato, A. Warshel, Exploring the origin of the ion selectivity of the KcsA potassium channel, Proteins 52 (2003) 412–426.
[263] S. Berneche, B. Roux, A microscopic view of ion conduction through the K^+ channel, Proc. Natl. Acad. Sci. U. S. A. 100 (2003) 8644–8648.
[264] S. Garofoli, P.C. Jordan, Modeling permeation energetics in the KcsA potassium channel, Biophys. J. 84 (2003) 2814–2830.
[265] P.C. Biggin, M.S. Sansom, Open-state models of a potassium channel, Biophys. J. 83 (2002) 1867–1876.
[266] A. Burykin, C.N. Schutz, J. Villa, A. Warshel, Simulations of ion current in realistic models of ion channels: the KcsA potassium channel, Proteins 47 (2002) 265–280.
[267] R.J. Mashl, Y. Tang, J. Schnitzer, E. Jakobsson, Hierarchical approach to predicting permeation in ion channels, Biophys. J. 81 (2001) 2473–2483.
[268] I.H. Shrivastava, M.S. Sansom, Molecular dynamics simulations and KcsA channel gating, Eur. Biophys. J. 31 (2002) 207–216.
[269] E. Perozo, D.M. Cortes, L.G. Cuello, Three-dimensional architecture and gating mechanism of a K^+ channel studied by EPR spectroscopy, Nat. Struct. Biol. 5 (1998) 459–469.
[270] Y. Liu, M. Holmgren, M.E. Jurman, G. Yellen, Gated access to the pore of a voltage-dependent K^+ channel, Neuron 19 (1997) 175–184.
[271] M. Zhou, J.H. Morais-Cabral, S. Mann, R. MacKinnon, Potassium channel receptor site for the inactivation gate and quaternary amine inhibitors, Nature 411 (2001) 657–661.
[272] Y. Jiang, A. Lee, J. Chen, M. Cadene, B.T. Chait, R. MacKinnon, Crystal structure and mechanism of a calcium-gated potassium channel, Nature 417 (2002) 515–522.
[273] M. Laine, M.C. Lin, J.P. Bannister, W.R. Silverman, A.F. Mock, B. Roux, D.M. Papazian, Atomic proximity between S4 segment and pore domain in Shaker potassium channels, Neuron 39 (2003) 467–481.
[274] B.E. Cohen, M. Grabe, L.Y. Jan, Answers and questions from the KvAP structures, Neuron 39 (2003) 395–400.
[275] C.E. Capener, P. Proks, F.M. Ashcroft, M.S.P. Sansom, Filter flexibility in a mammalian K channel: Models and simulations of Kir6.2 mutants, Biophys. J. 84 (2003) 2345–2356.
[276] M.A. Eriksson, B. Roux, Modeling the structure of agitoxin in complex with the Shaker K^+ channel: a computational approach based on experimental distance restraints extracted from thermodynamic mutant cycles, Biophys. J. 83 (2002) 2595–2609.
[277] V.B. Luzhkov, J. Nilsson, P. Arhem, J. Aqvist, Computational modelling of the open-state Kv 1.5 ion channel block by bupivacaine, Biochim. Biophys. Acta 1652 (2003) 35–51.
[278] I.T. Paulsen, M.K. Sliwinski, M.H. Saier, Microbial genome analyses: Global comparisons of transport capabilities based on phylogenies, bioenergetics and substrate specificities, J. Mol. Biol. 277 (1998) 573–592.
[279] C.F. Higgins, ABC Transporters—from Microorganisms to Man, Annu. Rev. Cell Biol. 8 (1992) 67–113.
[280] M.A. Bianchet, Y.H. Ko, L.M. Amzel, P.L. Pedersen, Modeling of nucleotide binding domains of ABC transporter proteins based on a F_1-ATPase/recA topology: structural model of the nucleotide binding domains of the Cystic Fibrosis Transmembrane Conductance Regulator (CFTR), J. Bioenerg. Biomembranes 29 (1997) 503–524.
[281] L.W. Hung, I.X. Wang, K. Nikaido, P.Q. Liu, G.F. Ames, S.H. Kim, Crystal structure of the ATP-binding subunit of an ABC transporter, Nature 396 (1998) 703–707.

[282] G. Chang, C.B. Roth, Structure of MsbA from E. coli: a homolog of the multidrug resistance ATP binding cassette (ABC) transporters, Science 293 (2001) 1793–1800.
[283] G. Chang, Structure of MsbA from *Vibrio cholera*: a multidrug resistance ABC transporter homolog in a closed conformation, J. Mol. Biol. 330 (2003) 419–430.
[284] K.P. Locher, A.T. Lee, D.C. Rees, The E. coli BtuCD structure: a framework for ABC transporter architecture and mechanism, Science 296 (2002) 1091–1098.
[285] K.P. Hopfner, A. Karcher, D.S. Shin, L. Craig, L.M. Arthur, J.P. Carney, J.A. Tainer, Structural biology of Rad50 ATPase: ATP-driven conformational control in DNA double-strand break repair and the ABC-ATPase superfamily, Cell 101 (2000) 789–800.
[286] P.M. Jones, A.M. George, Subunit interactions in ABC transporters: towards a functional architecture, FEMS Microbiol. Lett. 179 (1999) 187–202.
[287] J. Chen, G. Lu, J. Lin, A.L. Davidson, F.A. Quiocho, A tweezer-like motion of the ATP-binding cassette dimer in an ABC transport cycle, Mol. Cell 12 (2003) 651–661.
[288] P.C. Smith, N. Karpowich, L. Millen, J.E. Moody, J. Rosen, P.J. Thomas, J.F. Hunt, ATP binding to the motor domain from an ABC transporter drives formation of a nucleotide sandwich dimer, Mol. Cell 10 (2002) 139–149.
[289] J.D. Campbell, K. Koike, C. Moreau, M.S. Sansom, R.G. Deeley, S.P. Cole, Molecular modeling correctly predicts the functional importance of Phe594 in transmembrane helix 11 of the multidrug resistance protein, MRP1 (ABCC1), J. Biol. Chem. 279 (2004) 463–468.
[290] M. Seigneuret, A. Garnier-Suillerot, A structural model for the open conformation of the mdr1 P-glycoprotein based on the MsbA crystal structure, J. Biol. Chem. 278 (2003) 30115–30124.
[291] D.R. Stenham, J.D. Campbell, M.S. Sansom, C.F. Higgins, I.D. Kerr, K.J. Linton, An atomic detail model for the human ATP binding cassette transporter P-glycoprotein derived from disulfide cross-linking and homology modeling, FASEB J. 17 (2003) 2287–2289.
[292] J.D. Campbell, P.C. Biggin, M. Baaden, M.S. Sansom, Extending the structure of an ABC transporter to atomic resolution: modeling and simulation studies of MsbA, Biochemistry 42 (2003) 3666–3673.
[293] P.M. Jones, A.M. George, Mechanism of ABC transporters: a molecular dynamics simulation of a well characterized nucleotide-binding subunit, Proc. Natl. Acad. Sci. U. S. A. 99 (2002) 12639–12644.
[294] A.E. Senior, S. Nadanaciva, J. Weber, The molecular mechanism of ATP synthesis by F_1F_0-ATP synthase, Biochim. Biophys. Acta 1553 (2002) 188–211.
[295] J. Weber, A.E. Senior, ATP synthesis driven by proton transport in F_1F_0-ATP synthase, FEBS Lett. 545 (2003) 61–70.
[296] M. Yoshida, E. Muneyuki, T. Hisabori, ATP synthase—a marvelous rotary engine of the cell, Nat. Rev., Mol. Cell Biol. 2 (2001) 669–677.
[297] R. Yasuda, H. Noji, K. Kinosita, M. Yoshida, F_1-ATPase is a highly efficient molecular motor that rotates with discrete 120 degrees steps, Cell 93 (1998) 1117–1124.
[298] J.P. Abrahams, A.G.W. Leslie, R. Lutter, J.E. Walker, Structure at 2.8A resolution of F_1-ATPase from bovine heart mitochondria, Nature 370 (1994) 621–628.
[299] H. Noji, R. Yasuda, M. Yoshida, K. Kinosita Jr., Direct observation of the rotation of F_1-ATPase, Nature 386 (1997) 299–302.
[300] H. Wang, G. Oster, Energy transduction in the F1 motor of ATP synthase, Nature 396 (1998) 279–282.
[301] I. Antes, D. Chandler, H. Wang, G. Oster, The unbinding of ATP from F_1-ATPase, Biophys. J. 85 (2003) 695–706.
[302] R.A. Bockmann, H. Grubmuller, Nanoseconds molecular dynamics simulation of primary mechanical energy transfer steps in F1-ATP synthase, Nat. Struct. Biol. 9 (2002) 198–202.
[303] R.A. Bockmann, H. Grubmuller, Conformational dynamics of the F(1)-ATPase beta-subunit: a molecular dynamics study, Biophys. J. 85 (2003) 1482–1491.
[304] J. Schlitter, M. Engels, P. Kruger, E. Jacoby, A. Wollmer, Targeted molecular-dynamics simulation of conformational change—application to the T–R transition in insulin, Mol. Simul. 10 (1993) 291.
[305] J. Ma, T.C. Flynn, Q. Cui, A.G. Leslie, J.E. Walker, M. Karplus, A dynamic analysis of the rotation mechanism for conformational change in F(1)-ATPase, Structure 10 (2002) 921–931.
[306] W. Yang, Y.Q. Gao, Q. Cui, J. Ma, M. Karplus, The missing link between thermodynamics and structure in F_1-ATPase, Proc. Natl. Acad. Sci. U. S. A. 100 (2003) 874–879.
[307] M. Strajbl, A. Shurki, A. Warshel, Converting conformational changes to electrostatic energy in molecular motors: the energetics of ATP synthase, Proc. Natl. Acad. Sci. U. S. A. 100 (2003) 14834–14839.
[308] M. Dittrich, S. Hayashi, K. Schulten, On the mechanism of ATP hydrolysis in F_1-ATPase, Biophys. J. 85 (2003) 2253–2266.
[309] A. Aksimentiev, I. Balabin, R.H. Fillingame, K. Schulten, Insights into the molecular mechanism of rotation in the Fo sector of ATP synthase, Biophys. J. 86 (2004) 1332–1344.
[310] R. Koebnik, K.P. Locher, P. Van Gelder, Structure and function of bacterial outer membrane proteins: barrels in a nutshell, Mol. Microbiol. 37 (2000) 239–253.
[311] G.E. Schulz, The structure of bacterial outer membrane proteins, BBA-Biomembranes 1565 (2002) 308–317.
[312] J.D. Faraldo-Gomez, M.S. Sansom, Acquisition of siderophores in gram-negative bacteria, Nat. Rev., Mol. Cell Biol. 4 (2003) 105–116.
[313] D.P. Tieleman, H.J. Berendsen, A molecular dynamics study of the pores formed by *Escherichia coli* OmpF porin in a fully hydrated palmitoyloleoylphosphatidylcholine bilayer, Biophys. J. 74 (1998) 2786–2801.
[314] D.P. Tieleman, L.R. Forrest, M.S. Sansom, H.J. Berendsen, Lipid properties and the orientation of aromatic residues in OmpF, influenza M2, and alamethicin systems: molecular dynamics simulations, Biochemistry 37 (1998) 17554–17561.
[315] K.M. Robertson, D.P. Tieleman, The molecular basis of voltage gating of OmpF porin, Biochem. Cell. Biol. 80 (2002) 517–523.
[316] E.M. Nestorovich, T.K. Rostovtseva, S.M. Bezrukov, Residue Ionization and Ion Transport through OmpF Channels, Biophys. J. 85 (2003) 3718–3729.
[317] W. Im, B. Roux, Ion permeation and selectivity of OmpF porin: a theoretical study based on molecular dynamics, Brownian dynamics, and continuum electrodiffusion theory, J. Mol. Biol. 322 (2002) 851–869.
[318] K.M. Robertson, D.P. Tieleman, Orientation and interactions of dipolar molecules during transport through OmpF porin, FEBS Lett. 528 (2002) 53–57.
[319] A. Pautsch, G.E. Schulz, High-resolution structure of the OmpA membrane domain, J. Mol. Biol. 298 (2000) 273–282.
[320] A. Pautsch, G.E. Schulz, Structure of the outer membrane protein A transmembrane domain, Nat. Struct. Biol. 5 (1998) 1013–1017.
[321] S. Grizot, S.K. Buchanan, Structure of the OmpA-like domain of RmpM from *Neisseria meningitidis*, Mol. Microbiol. 51 (2004) 1027–1037.
[322] L.K. Tamm, F. Abildgaard, A. Arora, H. Blad, J.H. Bushweller, Structure, dynamics and function of the outer membrane protein A (OmpA) and influenza hemagglutinin fusion domain in detergent micelles by solutions NMR, FEBS Lett. 555 (2003) 139–143.
[323] P.J. Bond, J.D. Faraldo-Gomez, M.S. Sansom, OmpA: a pore or not a pore? Simulation and modeling studies, Biophys. J. 83 (2002) 763–775.
[324] P.J. Bond, M.S.P. Sansom, Membrane protein dynamics versus environment: simulations of OmpA in a micelle and a bilayer, J. Mol. Biol. 329 (2003) 1035–1053.

[325] H.J. Snijder, I. Ubarretxena-Belandia, M. Blaauw, K.H. Kalk, H.M. Verheij, M.R. Egmond, N. Dekker, B.W. Dijkstra, Structural evidence for dimerization-regulated activation of an integral membrane phospholipase, Nature 401 (1999) 717–721.

[326] M. Baaden, C. Meier, M.S.P. Sansom, A Molecular Dynamics Investigation of Mono and Dimeric States of the Outer Membrane Enzyme OMPLA, J. Mol. Biol. 331 (2003) 177–189.

[327] A.D. Ferguson, V. Braun, H.P. Fielder, J.W. Coulton, K. Diederichs, W. Welte, Crystal structure of the antibiotic albomycin in complex with the outer membrane transporter FhuA, Protein Sci. 9 (2000) 956–963.

[328] A.D. Ferguson, J.W. Hoffman, J.W. Coulton, K. Diederichs, W. Welte, Siderophore-mediated ion transport: crystal structure of FhuA with bound lipopolysaccharide., Science 282 (1998) 2215–2220.

[329] A.D. Ferguson, J. Kodding, G. Walker, C. Bos, J.W. Coulton, K. Diederichs, V. Braun, W. Welte, Active transport of an antibiotic rifamycin derivative by the outer membrane protein FhuA., Structure 9 (2001) 707–716.

[330] K.P. Locher, B. Rees, R. Koebnik, A. Mitschler, L. Moulinier, J.P. Rosenbusch, D. Moras, Transmembrane signalling across the ligand-gated FhuA receptor: crystal structures of free and ferrichrome-bound states reveal allosteric changes., Cell 95 (1998) 771–778.

[331] J.D. Faraldo-Gomez, G.R. Smith, M.S. Sansom, Molecular dynamics simulations of the bacterial outer membrane protein FhuA: a comparative study of the ferrichrome-free and bound states, Biophys. J. 85 (2003) 1406–1420.